A SYSTEMATIC ANALYSIS OF THE ROLE OF THE CYTOSKELETON IN *DROSOPHILA MELANOGASTER* MUSCLE MAINTENANCE

by

Alexander David Perkins

B.Sc.(Hons), The University of British Columbia, 2010

A THESIS SUBMITTED IN PARTIAL FULFILLMENT OF

THE REQUIREMENTS FOR THE DEGREE OF

MASTER OF SCIENCE

in

THE FACULTY OF GRADUATE STUDIES

(Cell and Developmental Biology)

THE UNIVERSITY OF BRITISH COLUMBIA

(Vancouver)

April 2013

Abstract

Animal muscles must maintain their function while bearing substantial mechanical loads and undergoing numerous contraction/extension cycles. How muscles withstand persistent mechanical strain is presently not well understood. The basic unit of muscle is the sarcomere, which is primarily composed of cytoskeletal proteins. I hypothesized that cytoskeletal proteins undergo renewal via protein turnover and that this is required to maintain muscle function. Using the adult flight muscles of the fruit fly, *Drosophila melanogaster,* I confirmed that the sarcomeric cytoskeleton undergoes turnover throughout the life of the organism. To uncover which cytoskeletal components are specifically required to maintain adult muscle function I performed an RNAi-meditated knockdown screen in adult *D. melanogaster* targeting the entire fly "cytoskeletome", the set of known cytoskeletal and cytoskeletal-associated proteins. Systematic gene knockdown was restricted to adult flies and muscle function was analyzed with behavioural assays. This approach identified 47 genes required for maintaining muscle function, 40 of which had no previously known role in this process. Detailed analysis of the role of candidate genes in adult muscles using confocal and electron microscopy showed that while muscle architecture was largely maintained after gene knockdown, maintenance of sarcomere length was disrupted. Specifically, I found that the ongoing synthesis and turnover of the key structural sarcomere component Projectin (*bent*) was required to maintain M-line integrity. Together, these results provide direct *in vivo* evidence of muscle protein turnover and identify possible roles for this process by uncovering specific functional defects associated with reduced expression of a subset of cytoskeletal proteins in the adult animal.

Preface

The work presented in this thesis has been submitted for publication as:

Perkins, AD, Lee, MJJ and Tanentzapf, G. (2013) A Systematic Analysis of the Role of the Cytoskeleton in *Drosophila melanogaster* Muscle Maintenance. PLoS Genetics (submitted).

This work was incorporated, with modifications, into Chapter 2, Chapter 3, and Chapter 4.

The work presented in Perkins et al, 2013 (submitted) was designed by ADP and GT. ADP conducted all the testing, with assistance from MJJL for the TARGET and Mef2::GAL4 screens. ADP and GT prepared the manuscript for publication.

Table of Contents

List of Figures

List of Abbreviations

Adenosine Triphosphate	ATP
Extracellular matrix	ECM
Dystroglycan Complex	DGC
Integrin adhesion complex	IAC
Indirect flight muscle	IFM
Longitudinal section	LS
Overnight	ON
Neuromuscular junction	NMJ
Phosphate buffered saline	PBS
Phosphate buffered saline with Tween-20	PBT
Room temperature	RT
Sarcoplasmic Reticulum	SR
Tergal Depressor of Trochanter	TDT
Transmission Electron Microscopy	TEM
Transverse section	TS

Acknowledgements

To Guy Tanentzapf, my supervisor. But for his chiding, erudition, unexpected kindnesses and ill-founded trust it would have been harder.

To my committee, Hugh Brock and Ed Moore. Their guidance, implicit deadlines, and encouragement gave focus when it was most needed. And to my examining committee, John Church and Doug Altshuler, for their time and thoughts.

To my colleagues, past and present, for indulging me. How could I help them, who could so little help myself?

My thanks to John Petkau and Tara Cai for their assistance with statistics.

To my family and friends for the brief moments of escape, continual – if ill deserved – support, and for being more proud of me than I could be. Especial thanks are due to Illtyd, Joanne, Norah, Edward, Felicity, Daniel, Aubrey, Sebastian and Connor. And to Stephanie. With her, I learned more than the work ever could have taught.

†

I've done it now, he managed to think. And without even telling them... He drew air into his lungs; if he could push it out again he'd be alright, but he couldn't, and everything faded out in a great roar of wordless voices.

- Kingsley Amis, *Lucky Jim*

Chapter 1: Introduction

Tissues in multicellular organisms are organized into highly ordered, three-dimensional structures that enable diverse and specific functions. Understanding the mechanisms by which tissues develop and maintain this complex architecture is a fundamental objective of cell and developmental biology. A major goal of cell biology is to understand how cell adhesion and the cytoskeleton allow tissues to obtain their architecture during development and then help maintain their shape for the duration of the life of the organism. Within this larger research goal, the work presented in this thesis aims to address the question of how tissue architecture is maintained in the adult animal. Cell adhesion and cytoskeletal proteins play important roles in the development of many tissues. As such, these classes are worthwhile subjects for further study in the context of muscle maintenance. However, their importance in tissue development inhibits study of their roles in maintenance as classic genetic loss of function approaches cause developmental defects that compromise the adult tissue. Muscles, the most common mechanism for multi-cellular force-generation in vertebrates and invertebrates, provide an excellent model for the study of tissue maintenance as they are both highly structured and long-lived [1]. This highly structured nature is typified by the sarcomere, the contractile apparatus that generates force for muscle contraction. The longevity is exemplified in vertebrates by cardiac muscles which can live for many decades [2] and in invertebrates by fly muscle cells which survive for the entire adult lifespan [3]. Technical advances in the fruit fly, *Drosophila melanogaster*, have allowed for the development of protocols to study the specific roles of cell adhesion and cytoskeletal proteins in tissue maintenance[4-7]. By harnessing these techniques, I have been able to systematically analyze the role of the cytoskeleton in muscle tissue architecture in ways that were previously not possible.

1.1 Muscles are a conserved force-generating mechanism common to most metazoan lineages

Muscles are the most common mechanism of force-generation in animals. Among other functions, muscles enable organismal locomotion, move food through the digestive system and power the heart. As such, they are one of the keystone components of animal life and are evolutionarily more distant than the divergence of the vertebrate and invertebrate lineages [8]. Muscles are divided into several distinct classes based on their function and appearance. In vertebrates, there are skeletal, cardiac and smooth muscles [8]. Vertebrate skeletal muscles are further subdivided into fast and slow skeletal muscles [9]. In invertebrates, muscle is classified as striated or smooth. Vertebrate skeletal muscle is analogous to invertebrate striated muscles and these muscles are used for organismal locomotion, under the control of the somatic (voluntary) nervous system [3,8]. Smooth muscles are controlled by the autonomic nervous system and regulate such biological activities such as the rhythmic contractions of the digestive system.

In this thesis, I focus on skeletal/striated muscles. To achieve organismal locomotion, muscles must be attached, via tendon cells, to either an endoskeleton (in vertebrates) or an exoskeleton (in invertebrates) [10]. While the position of the skeleton changes from vertebrates to invertebrates, the composition of the muscle fibres does not. Indeed, the mechanisms by which muscles work as well as their molecular composition are both highly conserved between vertebrates and invertebrates [1,8,11]. Thus, invertebrates are a powerful model system in which to study muscles.

1.1.1 Skeletal muscle structure

The basic units of muscle are the sarcomeres and sarcomeric architecture is conserved across the animal kingdom [1,8,11]. The sarcomere is an elaborate multiprotein complex of various cytoskeletal molecules including structural, linker and regulatory proteins that are precisely patterned to form contractile arrays (Figure 1.1 A-C) [1,12,13]. The core components of the sarcomere are myosin and actin; actin is anchored at the Z-disc while myosin molecules are anchored to each other at the midpoint between two adjacent Z-discs, in the M-line[1] (Figure 1.1 A). The giant protein Titin, the third most abundant protein in the sarcomere, binds to the Z-disc and extends into the M-line, Titin thus spans half the length of the sarcomere and acts as a molecular spring providing elasticity[14-16] (Figure 1.1 C). Many proteins surround and interact with actin and myosin to establish and maintain sarcomeric organization including nebulin and CapZ, which regulate the length of actin filaments in the muscle[17,18]; troponin, which regulates sarcomere contraction[19]; and tropomyosin, an actin binding molecule that regulates actin dynamics in the thin filaments as well as contraction [20] (Figure 1.1). The Z-discs links adjacent sarcomeres and connects the sarcomere to the muscle cell plasma membrane at sites called costameres and this allows transmission of contractile force to the extracellular environment. Costameres are multiprotein complexes that link the cell membrane to the surrounding extracellular matrix[21] and contain dystroglycan, sarcoglycan, as well as integrins and their associated cytoplasmic binding partners (Figure 1.1 B). Our knowledge of the composition of the sarcomeres is constantly evolving and new components are still being identified[13,22,23].

To form the myofibrils that span the large, multi-nucleate muscle cells, sarcomeres are arranged end-to-end, connected by shared Z-discs (Figure 1.1 A,B). Myofibrils terminate in a

specialized attachment known as the myotendinous junction (MTJ). The myotendinous junction connects the muscle cell to the tendon cell, via the extracellular matrix (ECM), and then to the skeleton [24]. This provides a physical link by which the force generated during contraction can be transmitted to the animal skeleton.

Muscle cells are highly specialized to enable the rapid spread of the depolarizing electrical impulse that induces contraction. This signal arrives at a specialized synapse between a motor neuron and the muscle cell known as the neuromuscular junction (NMJ). Because muscle cells are so densely packed with myofibrils, specialized invaginations of the cell membrane called transverse tubules (T-tubules), are required to help to quickly propagate the depolarizing signal throughout the cell [25] (Figure 1.1 A). Propagation of this depolarization releases calcium ions (Ca^{2+}) from the sarcoplasmic reticulum (SR). Ca^{2+} plays an essential role in mediating muscle contraction. In order for contraction to take place, myosin must be able to bind actin. However, in the absence of Ca^{2+} the binding sites for myosin on actin filaments are blocked by the Tropomyosin/Troponin complex [25]. One component of the Troponin complex, Troponin C, has a Ca^{2+} binding site. When Ca^{2+} binds Troponin-C, it induces a positional change of the Tropomyosin/Troponin complex, allowing myosin to bind to the actin filaments, and initiating contraction (Figure 1.1 C). In invertebrates, Ca^{2+} also causes a conformational shift in myosin light chains that enables contraction. Thus, in the presence of ATP, Ca^{2+} is the key regulator of muscle contraction [25].

Figure 1.1 Skeletal muscle structure

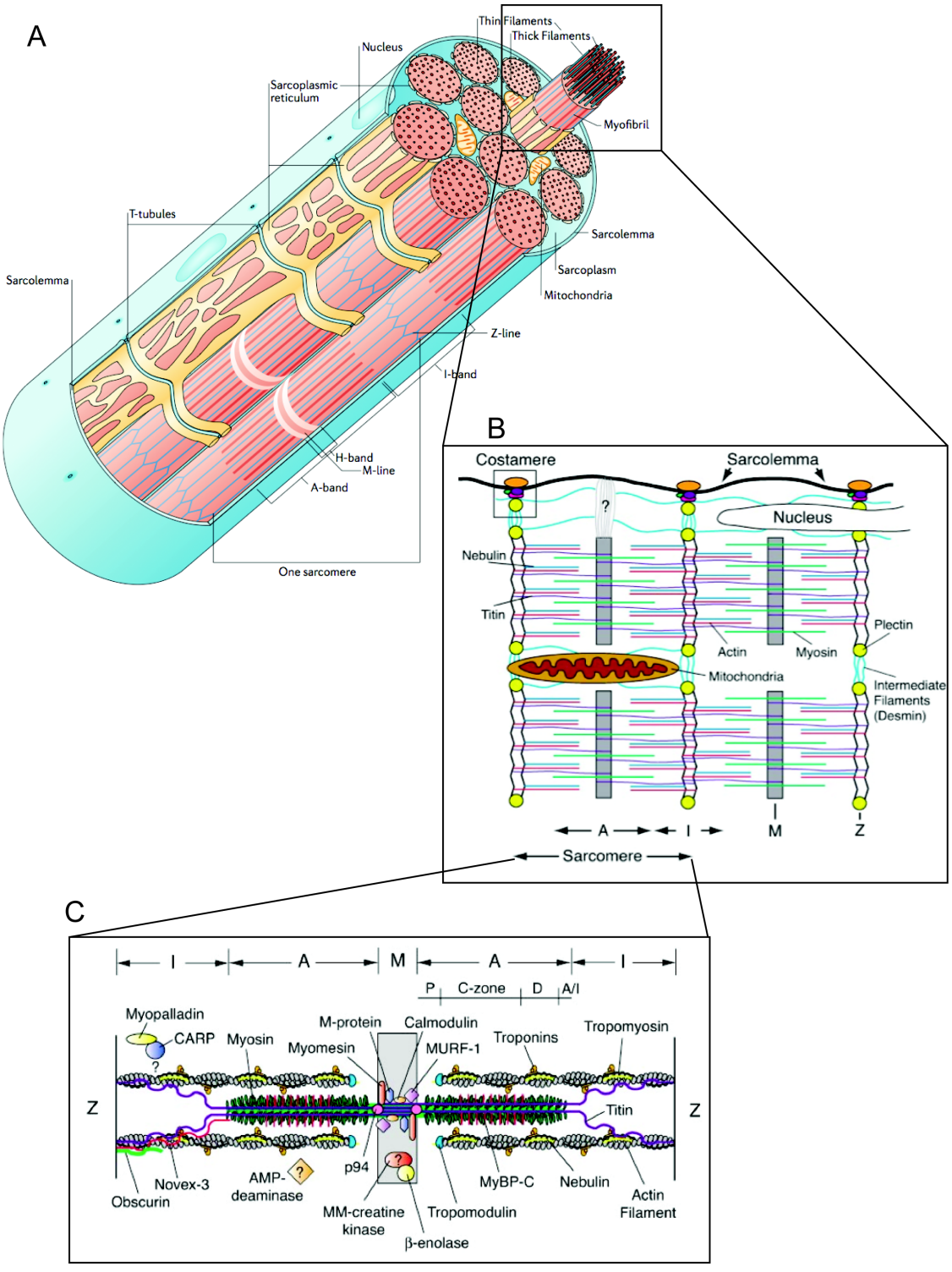

Figure 1.1 Skeletal muscle structure. Schematics of the molecular structure of skeletal muscles. (A) Myofibrils are bundled inside the muscle cell to form the contractile machinery. Myofibres contain sequentially linked sarcomeres (B). The sarcomeres are the basic unit of muscle. Sarcomeres are a multi-protein complex. Movement of myosin over the actin filaments creates muscle contraction. This interaction is mediated by the Tropomyosin/Troponin complex (C). (Figure 1.1 A Reprinted by permission from Macmillan Publishers Ltd: [NATURE REVIEWS MOLECULAR CELL BIOLOGY] Davies et al, 2006, copyright (2006); Figures 1.1 B and C Reprinted by permission from Annual Reviews Ltd: [ANNUAL REVIEW OF CELL AND DEVELOPMENTAL BIOLOGY] Clark et al, 2002, copyright (2002)).

1.1.2 The Drosophila musculature

The Drosophila musculature is specialized and distinct from vertebrate musculature in several ways. Firstly, *D. melanogaster* undergo two distinct rounds of myogenesis in their lifecycle. Secondly, *D. melanogaster* cardiac muscles are a specialized type of visceral muscle and as yet, no smooth muscles have been identified in *D. melanogaster* [3]. Thirdly, intermediate filaments are not present Drososphila muscles [26]. Finally, and most importantly for the work presented in this thesis, *D. melanogaster* muscles lack satellite cells, or at least no satellite cells have yet been identified [27]. Thus, *D. melanogaster* muscles do not possess the same regenerative capabilities of vertebrate muscles [3].

The first round of myogenesis in *D. melanogaster* occurs at the end of the embryonic phase of the lifecycle. Myogenesis is a multistep process involving myoblast specification and fusion; the guidance and attachment of the myotubes to tendon cells; and the organization of the cytoskeleton into sarcomeres and myofibrils [10,28,29]. In this first round of myogenesis, the muscles that will be used throughout the larval phase of the fly life cycle are formed. Most prominent among these muscles are the highly recognizable and well-studied somatic body wall muscles [10,30]. Indeed, this set of embryonic and larval muscles has bee an important model system for understanding the process of myogenesis [10,29,31,32].

The second round of myogenesis in flies occurs during metamorphosis. At this stage, nearly all the larval muscles are broken down and completely new, adult-specific, muscles are formed. These muscle cells last for the entire *D. melanogaster* lifespan. There are several muscle sets in adult *Drosophila*. The head contains the muscles that control head position and proboscis extension [33,34]. The thorax includes several important muscle sets: the indirect flight muscles (IFM), which power flight; and, the direct flight muscles, which provide control over flight

[34,35] (Figure 1.2 A). The leg contains the Tergal Depressor of Trochanter (TDT) muscle set that initiates the flight response by jumping and the leg muscles which power locomotion [36]. The main sets in the abdomen are the dorsal, lateral and ventral muscles which control abdomen movement and positioning [37] (Figure 1.2 A). Within the adult muscles there are two morphological types: fibrillar and tubular. The distinction is based upon arrangement of the actin/myosin complex, position of Z-discs and the SR [38]. In *Drosophila*, all muscles apart from the indirect flight muscles are tubular muscles [39].

The adult muscles of *Drosophila* have proven to be useful model systems for studying various aspects of muscle biology. The leg muscles have been used to study the second round of myogenesis [40,41] and the heart muscles have been used as a model for cardiac function [42,43]. However, the best-studied muscle set in the adult fly is the IFM [35,44,45].

1.1.2.1 The indirect flight muscle of adult flies

The IFMs are comprised two massive sets of fibrillar muscles, the dorsal ventral muscles and the dorsal longitudinal muscles that together power flight [46] (Figure 1.2). The IFMs are built from bundles of myofibrils, each consisting of sarcomeres (the basic contractile unit of muscle) lined up end-to-end. The IFMs are not required for viability and their function is easily assayed and thus they have become an important model system for the identification and characterization of essential muscle genes [45]. The contractions of IFMs occur at a frequency of ~200 Hz and move the wings through 170º of arc [46]. In order to achieve such a rapid contraction, IFM sarcomeres barely shorten during contraction [47]. The IFMs are asynchronous, which means that contractions are not timed to nervous impulses. The oscillating contractions that power flight are induced by a stretch activation from the TDT muscles [14]. As the IFMs

Figure 1.2 The indirect flight muscles (IFMs) of *Drosophila melanogaster*

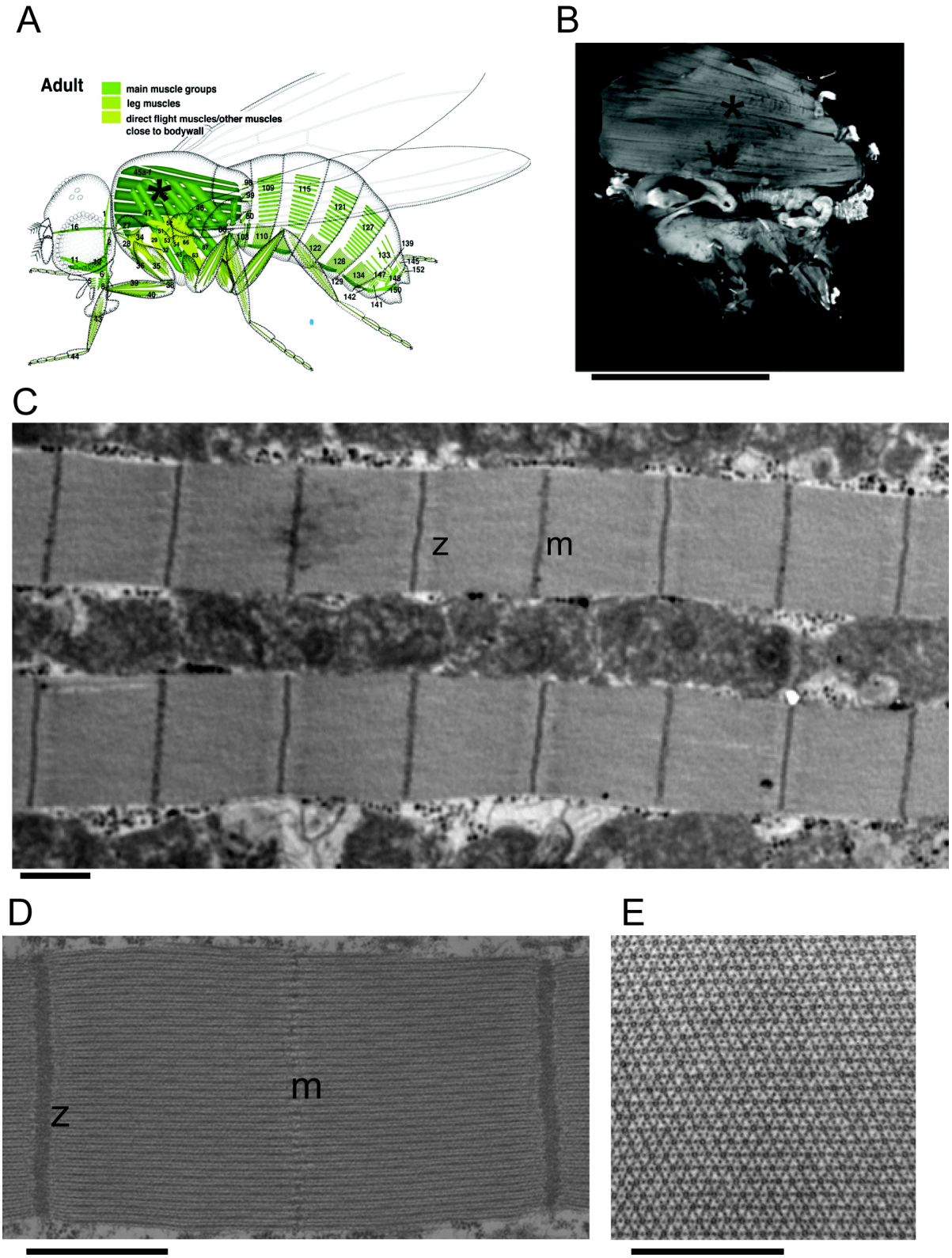

Figure 1.2 Schematic showing the indirect flight muscles (IFMs) of *Drosophila melanogaster.* Diagrammatic and microscopic representations of the *Drosophila* IFM. (A) Drawing of a whole fly showing the various muscle groups. Both sets of IFMs are indicated with an asterix. (B) Confocal micrograph of half a *Drosophila* thorax stained with phalloidin to label filamentous actin. The IFMs are marked with an asterix. Scale bar is 1mm. (C) Wide-angle electron micrograph of IFM myofibrils. Note sequential ordering of sarcomeres. z is Z-disc and m is M-line. Scale bar is 1µm. (D) Electron micrograph of a single sarcomere. Note interdigitation of thick and thin filaments. z is Z-disc and m is M-line. Scale bar is 1µm. (E) Transerve section of a myofibril showing a 1µm by 1µm square of myosin and actin filaments. Myosin filaments are the large circles, actin filaments are the smaller dots. Scale bar is 500nm. Panel (A) is adapted, with permission, from the Atlas of *Drosophila* Development, Volker Hartenstein, 1993.

undergo repeated, high-frequency contractions at close to the maximum power possible for fast twitch muscle relying on aerobic metabolism [46], their maintenance must be tightly controlled. Indeed, the IFMs of insects are thought to be some of the most powerful muscles in the animal kingdom [48]. However, as previously noted, no new muscles are formed after pupal myogenesis in *D. melanogaster* [3] and so the maintenance of existing muscles is key to their function.

1.1.3 *Drosophila melanogaster* as a model to study muscle

In summary, the fruit-fly, *Drosophila melanogaster*, provides an excellent model system in which to study muscles: there is no adult myogenesis in the fly, flies are amenable to genetic analysis, mutations in many sarcomeric components are available, fly sarcomeric proteins are well-conserved in relation to their vertebrate orthologs, and flies possess a number of well-characterized muscle types. As discussed, myogenesis in the fly is restricted to two phases of development and after pupal myogenesis no new muscles are made, so adult muscles must be maintained for the whole *D. melanogaster* lifespan [3]. Furthermore, the evolution of skeletal muscle predates the divergence of the vertebrate and invertebrate lineages [8]. Indeed, core sarcomeric components of fly muscles are, for the most part, well conserved in relation to vertebrates [8,11,49,50], making flies an excellent model in which gain insight into our own muscles. Genetic screens have identified loss-of-function mutations in the genes encoding all the major sarcomeric components [12,44,51], confirming the validity of fly muscles as a model for muscle.

1.2 Muscle maintenance

Given the repeated mechanical and chemical stresses muscle tissues are exposed to, muscles must work hard to maintain their function. Genetic analysis of long-term muscle maintenance has been a topic of intense study due to interest in both myodegenerative diseases and aging. Genes required for muscle maintenance have come either from studies in animal models or from cloning genes involved in human myodegenerative diseases. Two broad categories of genes have been identified for long-term muscle tissue maintenance: cytoskeletal and sarcomeric genes, and oxidative stress genes. The first category, cytoskeletal proteins, is discussed in detail in 1.4.2. The second category of mutations which affect muscle maintenance cause an increase in the rate of damage accumulation in muscle tissue and reveal themselves when muscle repair and renewal mechanisms are overwhelmed [3]. Such mutations typically impinge on oxidative stress homeostasis rather than the disruption of core contractile machinery [52]. Excess oxidative stress in the mitochondria of adult *D. melanogaster* muscles leads to myodegeneration [53,54]. Furthermore, disruptions to pathways that limit oxidative damage in mice exacerbate the effects of muscular dystrophy [55]. In humans, increased oxidative stress due to Vitamin E deficiencies [56] or defective antioxidase enzymes [57] are also linked with increased myodegeneration and muscular dystrophy [52].

1.3 *Drosophila* as a model for muscle disease

Apart from being an excellent model system in which to study basic muscle biology, *D. melanogaster* muscles have also been used as a model in which to study muscle disease as the genetic malleability of *D. melanogaster* allow far more elaborate and detailed analysis than is possible in vertebrate systems.

D. melanogaster has provided several insights into the mechanism underlying both Duchenne and Becker Muscular Dystrophy (DMD or BMD) which are caused by the loss or reduction of the dystrophin protein, respectively [51,58]. Dystrophin is a component of the Dystrophin-Dystroglycan Complex (DGC). The DGC is well-conserved in *Drosophila* [59]. Knockdown of the *dys* gene (which encodes Dystrophin) in *D. melanogaster* causes progressive muscle degeneration [60]. *D. melanogaster* has been established for limb-girdle muscular dystrophy, which is caused by a mutation to Sarcoglycan, another DGC component [61]. Another class of congenital human myopathies is caused by mutations to the ACTA1 gene. Such myopathies are characterized by severe disruptions to thin filament organization. A model for such myopathies in *D. melanogaster* has been successfully developed using mutations in the IFM-specific actin gene *act88F* [62]. Finally, Drosophila has been used extensively as a model for cardiac myopathies [42].

Beyond myofibrillar-specific myopathies, *D. melanogaster* is also used as a model for various neurodegenerative diseases including Parkinson's Disease (PD) and cardiac disease. A homolog of the *parkin* gene, which is linked to certain forms PD is exists in *D. melanogaster* making flies an attractive model for PD. Indeed, flies with *parkin* loss-of-function mutants show a mitochondrial pathology and apoptotic muscle degeneration similar to those observed in PD patients [53,54]. *D. melanogaster* has also been used to model various motor neuron diseases such as spinobulbar muscular atrophy, spinal muscular atrophy and amyotrophic lateral sclerosis [58].

1.4 The cytoskeleton in muscles

Cytoskeletal proteins are the primary structural components of myofibrils [1,12]. However, the cytoskeleton is not only important as a component of the sarcomere but has numerous other roles in muscle cells. Indeed, a recent genome-wide RNAi screen in *D. melanogaster* identified 2,785 genes required for muscle function and GO terms associated with the cytoskeleton ('Actin cytoskeleton' and 'Structural constituent of the cytoskeleton') were highly enriched within this set [63]. The cytoskeleton has several key roles: (1) it forms the contractile sarcomeric cytoskeleton, which contains the actin and myosin filaments; (2) it anchors and regulates the myofilaments; (3) it links and coordinates adjacent myofibrils; and (4) connects myofibrils to the cell membrane and ECM [64] (Figure 1.1 B, C). Specifically, actin and intermediate filaments work to shape the highly specialized structures of the NMJ and MTJ [1]. The microtubule arrays of striated muscles have many functions including the positioning organelles in muscle cells [1], providing a scaffold during muscle development [65], and supporting overloaded cardiac muscles [66]. In summary, the cytoskeleton fulfills numerous, diverse functions within muscles and is important during both muscle development and muscle maintenance.

1.4.1 The cytoskeleton is key to muscle development

The cytoskeleton is essential for a number of processes that are vital to muscle development [67]. During myogenesis, myoblasts fuse to form a syncytial myotube that elongates in a targeted manner to form muscle-tendon attachments. During the first step, myoblasts must assume a bipolar morphology in order to fuse with other myoblasts and the actin cytoskeleton is vital to this process [67]. As the myotube grows, it is directed towards its correct

binding sites with other muscles or with tendons and throughout this process the actin and microtubule cytoskeleton are required for cell migration and attachment to the adjacent muscle or tendon cells [10]. Myofibrillogenesis begins during myotube elongation [29]. During myofibrillogenesis, the role of the cytoskeleton is twofold. Firstly, as discussed previously, the cytoskeletal proteins are the key structural elements of myofibrils. Indeed, two cytoskeletal proteins, actin and myosin, are the most abundant proteins in muscle fibres forming the thin and thick filaments respectively [1]. Additionally, several other cytoskeletal proteins such as Titin, the third most abundant protein in muscles [68], Nebulin and α-Actinin are integral parts of sarcomere structure [1] (Figure 1.1 B, C). Secondly, the cytoskeleton assists in the assembly myofibrils by providing the scaffolding required to position the constituent parts of the sarcomere [69]. Currently, the accepted model for sarcomere assembly involves the independent assembly of multiple protein complexes that are then combined to form the sarcomere. Although not directly involved in the sarcomere, parts of the cytoskeleton are required to position these complexes [12].

1.4.2 Known roles for cytoskeletal proteins in maintaining muscle function and structure

Work in genetic model organisms such as *C. elegans* and *D. melanogaster* has been useful in highlighting the importance of several cytoskeletal components of the sarcomere in maintaining the adult musculature [3,51]. Studies using hypomorphic alleles of the sarcomeric proteins Myosin Heavy Chain (Mhc) [70], Flightin [71,72] and Troponin T [73] as well as mutational analysis of the costameric components Sarcoglycan [61], Dystroglycan and Dystrophin [74], and integrin [75] have shown that these genes play essential roles in maintaining muscle function. Genetic analysis of human patients also identified a number of

cytoskeletal and sarcomeric genes as being required for adult muscle function: mutations in actin, Troponin, Tropomyosin, Myosin and Nebulin have been implicated in congenital myopathies [76]. Moreover, mutations in the proteins Myotilin and Titin cause limb-girdle muscular dystrophy 1A and tibial muscular dystrophy respectively [77,78]. Thus, it is evident that the cytoskeleton is an important player in muscle maintenance. However, no systematic study of its role has previously been undertaken.

1.4.3 Cytoskeletal protein turnover in muscles

Throughout their lifetime, muscles endure continual mechanical strain [7,79,80] and the question arises as to what mechanisms exist to ensure that tissue integrity is maintained. One proposed mechanism is the ongoing turnover of sarcomeric components[53,55,56,81,82]. This hypothesis posits that mechanical tension damages the contractile machinery in muscles and that damaged proteins need to be replaced with newly made proteins[53,55,56,81,82]. A great limitation of these studies is that they have been restricted to observing turnover either in cultured muscle cells or, for very short time frames, in immobilized tissues *in vivo*. Additionally, these studies have been purely descriptive, and the question of whether turnover is functionally relevant has not been explored. Therefore, although we currently have convincing evidence that sarcomeric proteins undergo turnover, this process is poorly understood on a mechanistic and functional level. Specifically, it is unknown how widespread protein turnover is in the muscular cytoskeleton and to what extent this turnover is required to maintain muscle structure and function.

1.5 Genes required for muscle maintenance are also required in muscle development

Although mutations that affect muscle function in the adult have been previously identified (see 1.3.2), it is presently unclear whether these phenotypes are due to defects in muscle maintenance. In many cases it is likely that the defects in fact occur during myogenesis and are only revealed during adulthood [74,83-86]. Thus, the main problem in studying how adult muscle structure and function is maintained lies in describing functions in fully formed muscles for genes whose activity is required to form muscles in the first place [63,70-73]. Importantly, this issue has prevented the execution of a systematic screen to identify genes that are specifically required for the long-term maintenance of muscle function in the adult. This is despite the fact that a comprehensive RNAi screen was used to define the complete set of genes required for *D. melanogaster* muscle function, as this screen used an approach which knocked-down genes throughout development [63]. We have circumvented this problem by using temporal and tissue specific expression of RNAi transgenes to limit knockdown to adult flies (Figure 3).

1.6 Rationale, objectives and hypotheses

Based on the background literature, I designed a research project based on the following rationale, objectives and hypothesis. This thesis aims to report the methodology, findings and conclusions of this work.

1.6.1 Rationale

(1) *Drosophila* muscles are an excellent model system in which to study muscle maintenance

The adult fly musculature, and the IFMs in particular, provides a powerful model system for studying muscle maintenance since it is post-mitotic; easily accessible for mechanical, physiological and behavioral assays; placed under constant mechanical stress; and, amenable to many different genetic techniques.

(2) The cytoskeleton is an ideal candidate for to identify genes required for muscle maintenance

The cytoskeleton provides an attractive set of candidate genes to study in the context of muscle maintenance. The cytoskeleton plays multiple, important roles during muscle development and is required during muscle maintenance. However, technical limitations have previously prevented the systematic analysis of the role of the cytoskeleton in muscle maintenance.

1.6.2 Objectives

The thesis has three primary objectives:

(1) To understand the role that cytoskeletal protein turnover plays in maintaining adult muscle function.

(2) To define a set of cytoskeletal genes required for muscle maintenance.

(3) To characterize a subset of these genes to understand how they work to maintain muscle structure and function.

1.6.3 Hypotheses

Based on the background information and objectives, I formulated the following hypotheses:

(1) I hypothesize that cytoskeletal protein turnover is required to maintain adult muscle function.

(2) Inhibition of protein turnover in adult muscles, via RNAi-mediated, knockdown of cytoskeletal genes, will result in defects in muscle function.

(3) Core sarcomeric proteins are required to maintain muscle structure in adult animals.

Chapter 2: Materials and methods

2.1 Fly stocks and genetics

The cytoskeletal RNAi library was made up of lines sourced from the Vienna *Drosophila* RNAi Center (VDRC; [4]), the Harvard Transgenic RNAi Project (TRiP; [6]) and the National Institute of Genetics (NIG-Fly, Kyoto, Japan). The library was assembled based on bioinformatics analysis of the fly genome to identify components of the cytoskeleton [87]. Additional lines were included based on previously defined roles in muscle development. Finally, a control set of genes with no known muscle function or cytoskeletal role was included. The complete list of genes included in the RNAi library is given in Appendix C1. Al RNAi lines expressed short hairpin constructs under UAS control. For all TARGET experiments males homozygous for each UAS-RNAi line were crossed to females of the genotype *P[tubP-GAL80ts]9/FM7;;Mef2:GAL4/TM3*. The F1 progeny was raised at 18ºC until eclosion at which point virgin females were collected and transferred to 29ºC to induce RNAi expression. For the Mef2::GAL4 screen, UAS-RNAi males were crossed to females with the genotype $y^{1},w^{*};;P[GAL4\text{-}Mef2.R]3$. Actin turnover experiments were performed using a UAS-*act88F* GFP fusion line (Bloomington ID #9253) [88] and a UAS-eGFP line (Bloomington ID #6874).

2.2 The TARGET and Mef2::GAL4 systems

Throughout this thesis, two systems were used to express transgenic elements. The Mef2::GAL4 system limits the expression of the UAS binding protein GAL4 to muscles [7]. Mef2, Myocyte Enhancing Factor 2, is expressed only in muscle cells throughout all stages of fly

life. Thus, we are able to limit expression of transgenes under UAS control to muscles. For a graphical representation of the TARGET system, see Figure 2.1.

The TARGET system refers the Temporal And Regional Gene Expression Targeting system [5]. By combining the Mef2::GAL4 system with a temperature sensitive allele of the GAL4 inhibitor GAL80, we are able to control expression of a UAS transgene, or RNAi construct. At 18ºC, the GAL80 protein is functional and can inhibit GAL4/UAS-mediated transgene expression (Figure 2.2 A). At 29ºC, the GAL80 protein is denatured and can no longer inhibit GAL4/UAS transgene expression thus allowing expression of what genetic construct is under UAS control (Figure 2.2 B). We applied this system to express Act88F::GFP and eGFP in the Actin turnover experiments (See 3.2) as well as the RNAi constructs in the TARGET screen (See 3.4 and 3.5).

2.3 Electron microscopy

Fly muscles were prepared as follows. Thoraces were bisected and immediately placed in 2.5% glutaraldehyde, 1.6% paraformaldehyde with 0.1M sodium cacodylate buffer for 2 hours at room temperature (RT) (EMS, Hatfield, PA). Thoraces were washed in 0.1M sodium cacodylate for 4x 15 minutes. Thoraces were post-fixed for 2 hours at RT in 1% osmium tetroxide in 0.1M sodium cacodylate (EMS, Hatfield PA). Samples were dehydrated with an ethanol series and embedded in a 1:1 Spurr's and Embed812 mixture (EMS, Hatfield PA). Ultrathin silver-gold sections (85 nm thick) were cut using a Leica Ultramicrotome and 2mm ultra 45º DiATOME diamond knife (Leica Microsystems, Richmond Hill, ON; DiATOME, Biel, Switzerland). Sections were mounted on 200 mesh copper grids (EMS, Hatfield PA) and were double stained with

Figure 2.1 The Mef2::GAL4 system

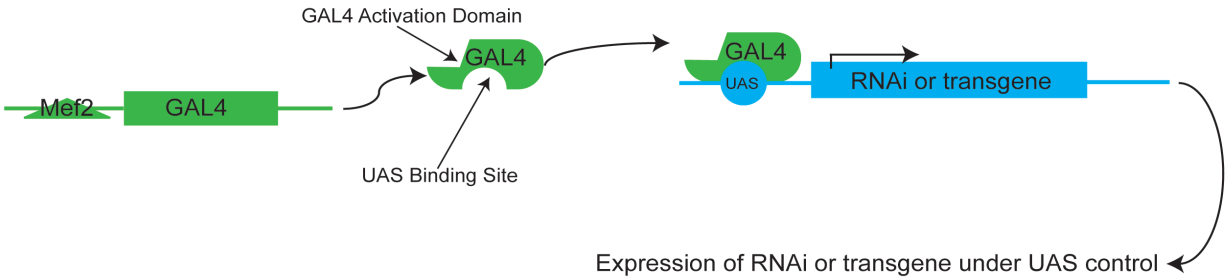

Figure 2.1 The Mef2::GAL4 system. The Mef2::GAL4 system enables muscle specific expression of the transcription activator protein GAL4. GAL4 binds the UAS promoter sequence and recruits the necessary transcriptional machinery to express whatever genetic element is downstream of the UAS sequence. In this thesis, this would be a GFP transgene or an RNAi construct.

uranyl acetate and lead citrate for 4 minutes each. Electron micrographs were obtained using a transmission electron microscope (FEI Tecnai G2 Spirit, FEI, Hillsboro, OR).

2.4 Immunohistochemisty and confocal microscopy

Antibody staining was performed as previously described [75] with modifications. Fly thoraces were bisected to expose the IFMs. Thoraces were then fixed in 4% paraformaldehyde in PBS for 20 minutes at RT, rinsed with fresh PBT 3x, incubated for 1 hour in PBT and blocked in 0.2% BSA for 1 hour at RT. Thoraces were incubated with primary antibodies overnight (ON) at 4ºC, washed, blocked in BSA and incubated ON at 4ºC with secondary antibodies. IFMs were dissected out and mounted on glass slides. For phalloidin staining, thoraces were fixed in 4% paraformaldehyde in PBS for 20 minutes at RT, rinsed with fresh PBS 3x, washed for 1 hour in PBS then incubated ON at 4ºC. The primary antibodies used were anti-obscurin (pAb rabbit, 1:200, gift of Dr. Belinda Bullard) and anti-a-actinin (MAC276, rat mAb, 1:200, gift of Dr. Belinda Bullard). Phalloidin was conjugated to Alexa Fluor 488 or rhodamine-phalloidin (Invitrogen). Confocal images were obtained using an Olympus IX81/FV1000 microscope with 10x/0.40, 40x/1.30 oil and 60x/1.33 oil objectives. Images were processed with Adobe Photoshop and ImageJ.

2.5 Quantification of sarcomeric parameters

To more closely study how aging muscles over 30 days or after RNAi knockdown of *act88F*, *mhc* or *bent* altered sarcomere dimensions, we quantified various sarcomeric parameters as described in 2.5.1-3.

Figure 2.2 The TARGET system

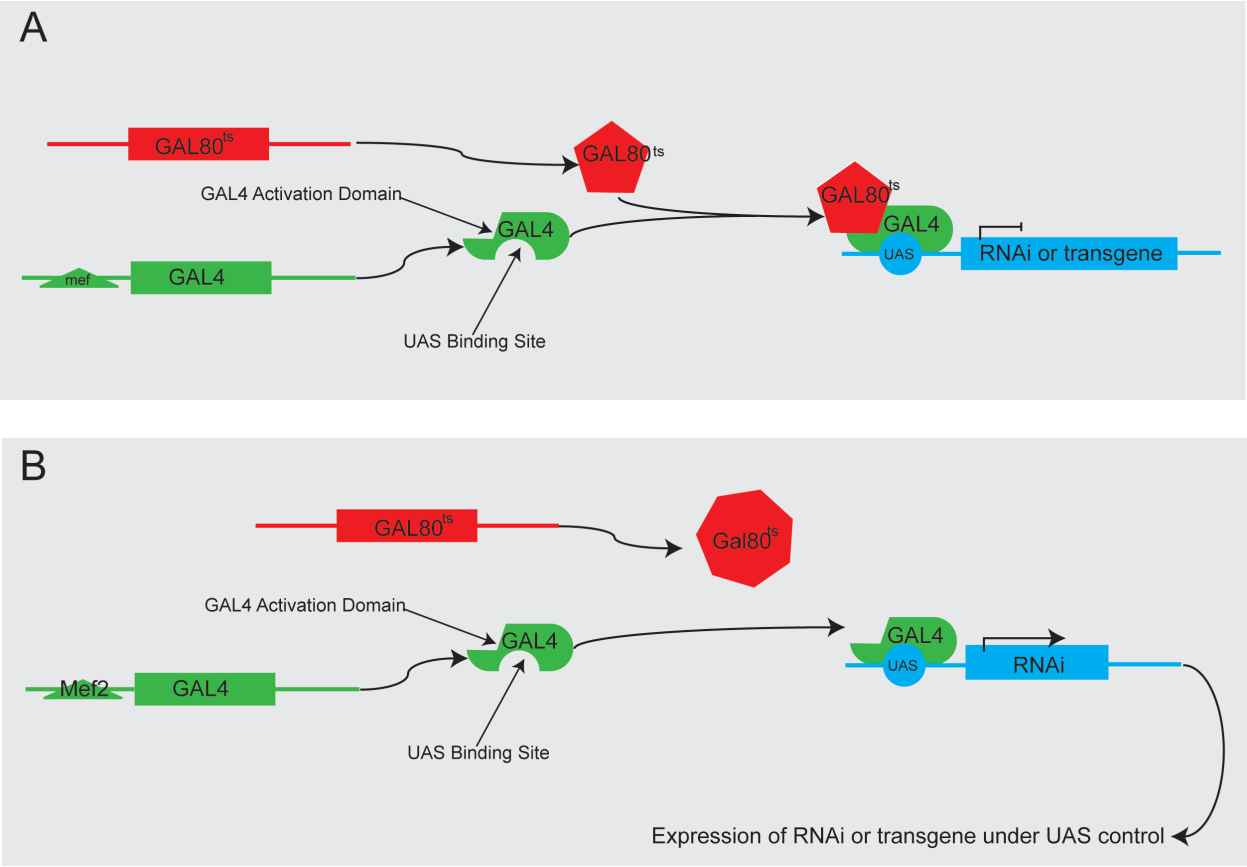

Figure 2.2 The TARGET system. Schematic representation of the TARGET system. As in the Mef2::GAL4 system, the Mef2 promoter is used to express GAL4 in muscle cells. In the TARGET system, a temperature sensitive allele of the GAL4 inhibitor GAL80 is added. (A) At 18ºC, the GAL80 protein can assume its correct conformation and binds GAL4 at the Activation Domain thus blocking recruitment of transcriptional machinery. (B) At 29ºC, the conformation of GAL80 altered, preventing its inhibition of the GAL4 Activation Domain. Thus, whatever genetic element is downstream of the UAS promoter is transcribed.

2.5.1 Sarcomere length quantification from electron micrographs

Sarcomere length was calculated in as follows. Electron micrographs were prepared as detailed above. ImageJ was used to measure the Z-disk-to-Z-disk distance of the IFM sarcomeres. Only sarcomeres located in myofibrils in the same plane as the section were included. For each data point, a total of at least 20 sarcomeres from at least 2 different animals were counted. Samples were fixed in parallel to eliminate fixation artifacts in the length of sarcomeres. For the knockdown experiments, sarcomere length was normalised to the pre-RNAi induction time point to allow the changes to be compared between samples. Sarcomere length was measured using ImageJ. Statistical comparison was performed using the Student's T-test in the statistical analysis software Prism (Graphpad, La Jolla CA).

2.5.2 Quantification of myosin packing density

Myosin filament density was calculated as follows. Cross-sections of the IFMs clearly displaying the hexagonal lattice of myosin and actin filaments were cropped to 1μm by 1μm areas. Myosin filaments were counted for at least 8 cross-sections per time-point or genotype and then averaged. These counts provided the filament packing density (number of filaments/μm^2). Time points were compared using the Student's T-test in the statistical analysis software Prism (Graphpad, La Jolla CA).

2.5.3 Sarcomere length, thin filament length and M-line width quantification

Profiles of sarcomeric actin were produced as follows. IFM sarcomeres were stained with phalloidin as described above. Intensity profiles were measured from Z-disc to Z-disc using ImageJ (see Figure 3.11 A and A'). Overall sarcomere length was calculated as an average of Z-disc/Z-disc distances for a sample of sarcomeres. Thin filament length was calculated as the distance from the Z-disc to halfway down the fluorescent intensity slope to the M-line. M-line width was calculated as the distance between the end of one thin filament array to the beginning of the adjacent array (Figure 3.11 A and 3.11 A'). Lengths were compared using the Student's T-test in the statistical analysis software Prism (Graphpad, La Jolla CA).

2.6 Negative geotaxis assays

Geotaxis assays were carried out as previously described [75,89] with modifications. Flies were collected after eclosion and separated into batches of 10 in vials containing a standard food medium. For the climbing assay, the flies from one vial were transferred to an empty vial. Flies were tapped to the bottom and the number flies that climbed 7.5 cm in 8 seconds was recorded. Each vial was tested 5 times in immediate succession. For each experimental line, approximately 4 replicate vials of 10 flies were tested at each time-point. The climbing index is the ratio of a given data point to the score recorded prior to the shift to the permissive temperature of 29ºC. Each replicate vial of 10 flies was assayed every 3 days for 30 days. Environmental conditions (e.g.: light, humidity, temperature, food) were kept constant for all the experiments. The assays were carried out in the early afternoon when flies are active.

2.6.1 Statistical modeling of negative geotaxis assay data

Statistical analysis of the data was carried out as follows. I used a second-order model to fit the data generated from the geotaxis assays. I used the Generalized Estimating Equations (GEE) approach to estimate the coefficient values (X, Y and Z) for the following quadratic equation.

(1) $$P_{jk} = e^{(X+Y*Day+Day^2)}$$

This equation calculated *P,* where *P* is the probability of climbing above the 7.5cm line after 8 seconds (see section on the Negative Geotaxis Assay) for a fly with genotype *j* on Day *k* following RNAi knockdown. I validated the model by comparing the predicted probability for a given day to the experimental data. To analyze the data, an odds ratio was calculated by finding the ratio of the log of the probability, the odds, for the wild-type control and RNAi line at a given day. An odds ratio not significantly different from '1' indicated no difference between the RNAi line and control line. The advantage of analyzing my data in this way was that it allowed me to include all the data for a given RNAi knock-down line when calculating the probability for a specific time-point as the GEE approach includes the entire dataset when generating the X, Y and Z coefficients for Equation 1. Furthermore, this analysis approach was optimized for data sets where the decline in P_{jk} is gradual. The statistical analysis was performed using the statistical analysis software R (www.r-project.org).

2.7 Quantitative PCR

Total RNA was isolated from >5 flies per experiment using TRIzol (Invitrogen). 1000ng of total RNA was converted to cDNA using the qScript cDNA Synthesis Kit (Quanta

BioSciences). qPCR was performed using the PerfeCta SYBR Green FastMix, ROX kit (Quanta Biosciences) with the primer pairs: 5'-TGAAGCCAGATTCAGCAAACCC-3' and 5'-TACTGCCGGTAAACACCTCGTC-3' for *bent*; 5'-ATGTCCGACGATGAAGAGTACACC-3' and 5'-CTTCTGGTCCTGACGCTTGATG'3' for *mhc*; and 5'-AACTCGATCATGAAGTGCGACGTG-3' and 5'-CTGCATACGATCGGCAATACCAG-3' for *act88F*. GAPDH mRNA levels were assayed as an internal control using the primer pair: 5'-AAAGCGGCAGTCGTAATAGC-3' and 5'-GACATCGATGAAGGGATCGT-3'. Changes in expression were calculated using the comparative Ct method [90]. For the wild-type profile, at least 3 separate extractions (each of >10 flies) of total RNA were measured independently for each time point. For knockdown confirmation in *bent*, *mhc* or *act88F* RNAi flies at least 2 separate extractions using >5 flies of RNA per time-point were performed. Differences in mRNA levels were analysed using t-tests and the statistical analysis software Prism (Graphpad, La Jolla CA).

2.8 Actin turnover analysis

A GFP-tagged Actin88F (Act88F::GFP) construct was obtained from the Bloomington Stock Center. Using the TARGET system, Act88F::GFP was induced post-eclosion in adult muscles (Figure 2.2; Figure3.2). To track incorporation of Act88F::GFP into sarcomeres, a pulse-chase experiment was performed. Act88F::GFP was pulsed by moving flies to 29ºC post-eclosion (Figure 3.2 A). Optimization of the pulse-chase experiment determined that 28 hours was the ideal length for the pulse. Longer pulses of Act88F::GFP expression resulted in saturated level Act88F::GFP such that a decline in fluorescent intensity could not be observed. Shorter pulses did not allow fluorescence intensity reach the maximum as identified by continuous

expression of Act88F::GFP. After the 28 hour pulse of Act88F::GFP, flies were returned to 18ºC to limit Act88F::GFP expression. As a control, I also expressed a cytoplasmic UAS-eGFP (eGFP) under the same conditions. IFMs were dissected from fly thoraces and fixed ON at 4ºC in 4% formaldehyde in 1x PBS and stained with rhodamine phalloidin to highlight sarcomeres.

2.8.1 Quantification of Z-disc intensity

To assess fluorescence intensity in the muscle for both eGFP and Act88F::GFP, I quantified fluorescent intensity at the Z-discs as indicated by the rhodamine-phalloidin staining. Using ImageJ, a irregular rectangle (drawn to best fit the Z-disc) was placed around the Z-disc and the average pixel intensity inside it was quantified. This was repeated at least 40 times for Z-discs in different IFM sets and multiple animals. The measurements were then averaged and graphed. This approach enabled us to quantify the extent to which eGFP or Act88F::GFP was entering the muscle fibres.

2.8.2 Quantification of the ratio of intensity at the Z-disc to the sarcomere body

To determine the specificity of the eGFP or Act88F::GFP incorporation to the Z-disc, I calculated the ratio of the intensity at the Z-disc compared to the adjacent sarcomere body. The adjacent sarcomere body was defined as a whole sarcomere neighbouring a given Z-disc, less the Z-discs. This allowed us to assess the primary location of incorporation. Z-disc intensity measurements were performed as in 2.8.1 and sarcomere body intensity measurements were obtained in a similar manner. For both 2.8.1 and 2.8.2, images were processed with ImageJ, and the data was processed using Prism (Graphpad, La Jolla CA).

2.9 Bioinformatic analysis

Genes included in the screen were assigned broad functional terms based on terms mined from the Gene Ontology (www.geneontology.org) and FlyBase (www.flybase.org). Genes were grouped by two criteria: muscle and cytoskeletal. The term 'Muscle' was assigned if the gene had a previously known role in any part of muscle development, function or maintenance. Otherwise, the term 'Miscellaneous' was assigned. Additionally, genes were classed as 'Cytoskeletal' or 'Non-cytoskeletal' based on GO terms and previous bioinformatic analysis of the *D. melanogaster* genome to identify cytoskeletal components [87].

2.9.1 Heatmap generation

For heatmaps, enrichment of GO terms was calculated using the AmiGO GO Term Enrichment Tool. The frequency of a specific GO term appearing in a phenotypic set was compared to the frequency of the same term appearing in the entire screen to generate an Enrichment Ratio (ER). These ERs where then used to generate a heatmap. Heatmaps were produced using R (www.r-project.org). For more detail on how heatmaps were generated, see Appendix A.

Chapter 3: The identification and characterization of genes required for muscle maintenance

3.1 Adult fly muscles exhibit ongoing transcription of sarcomeric proteins and subtle changes over time

During aging, fly muscles undergo characteristic changes including: Z-disc disruption/fragmentation, reduction in the expression of sarcomeric components, loss of thin filament organization, and reduced flight and climbing ability. However, these studies focused on flies towards the end of their lifespan [91]. To test whether muscles also undergo changes earlier in life, I investigated muscle morphology, function, and sarcomeric protein expression prior to the time at which aging-associated defects appear. Electron microscopy was used to analyze the ultrastructure of the IFM at 6-day intervals following eclosion. Longitudinal and transverse sections revealed no obvious changes in sarcomeric architecture between Day 0 and Day 30 (Figure 3.1 A-C). However, rigorous quantitative analysis of sarcomere length and packing density revealed subtle variations over the 30-day time-course. Sarcomere length temporarily declined post-eclosion, from Day 6 to Day 18, before returning to its initial length by Day 30 (Figure 3.1 B and D). Analysis of myosin packing density showed that filament density fluctuated over a 30-day period post-eclosion (Figure 3.1 C and E). This illustrates that muscle architecture is dynamic.

Figure 3.1 Wild-type adult muscles are a dynamic tissue

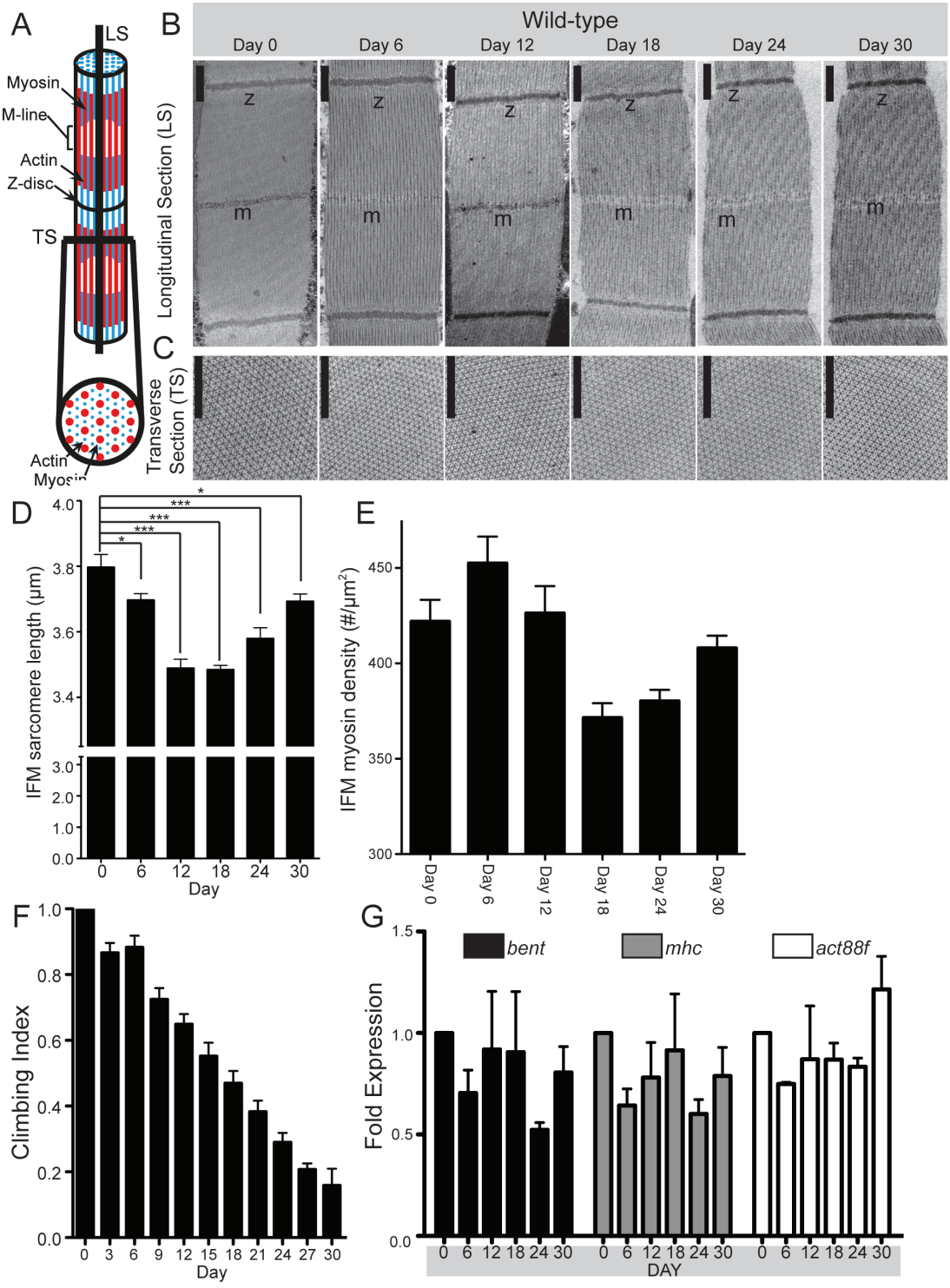

Figure 3.1 Wild-type adult muscles are a dynamic tissue. Morphology, function and transcriptional activity of wild-type IFMs were assayed at sequential time points during the first 30 days of fly life. (A) Schematic of myofibril showing two sarcomeres. Red lines are myosin (thick) filaments and blue lines are actin (thin) filaments. Z-disc and M-lines are indicated. A transverse view is provided below. LS is Longitudinal Section. TS is Transverse Section. (B) LS and (C) TS of wild-type IFM sarcomeres show that the Z-disc or M-lines, actin and myosin filaments, and the myosin and actin lattice all exhibit consistent appearance over the first 30 days of fly life. (B: z, Z-disc. m, M-line; C: Larger circles are myosin, smaller dots are actin; Scale bars are 500nm). (D) Sarcomere length fluctuates over 30 days. Sarcomere length was measured Z-disc to Z-disc using electron micrographs. At all time-points length was significantly reduced compared to Day 0. (E) Quantification of myosin filament density in transverse sections of wild-type IFMs. (F) Climbing ability of adult flies decreases over 30 days. Climbing ability was measured using a negative geotaxis assay. Over 30 days, climbing ability decreased by 85%. (G) Key sarcomeric genes are continually transcribed. qPCR was used to assay for expression of *bent*, *mhc*, and *act88F*. For all three genes, mRNA levels were maintained, with slight variations, over the first 30 days fly life. For all panels, error bars indicate standard error; * indicates a p-value<0.05, ** indicates a p-value<0.005, *** indicates a p-value<0.0005. For (D) N≥30 individual sarcomeres from different muscles from multiple flies. For (E) N≥3000 myosin filaments/time-point (>10 IFM transverse sections) from multiple flies. For (F) N=60 flies. For (G) N≥3 independent RNA extractions using >10 flies for each time-point were performed.

Next, I assayed muscle function over the first 30 days post eclosion using a classic behavioral assays to test climbing ability and observed a functional decline starting at eclosion. Negative geotaxis climbing assays showed an 82% decline in climbing ability over 30 days (Figure 3.1 F).

We then tested whether the transcription of core sarcomeric proteins varied during the fly lifespan using quantitative PCR (qPCR) to study mRNA levels of *bent* (Titin), *mhc* (muscle Myosin), *act88F* (Actin) at 6-day intervals. All three core sarcomeric proteins were continuously transcribed at similar levels from eclosion until Day 30 (Figure 3.1 G). Taken together my data reveal that during the first 30 days of fly life muscles are a dynamic tissue; in particular the ongoing transcription of sarcomeric proteins suggests that these structures undergo renewal.

3.2 Actin undergoes *in vivo* turnover in adult muscles

As the qPCR analysis showed persistent expression of sarcomeric actin during fly life, we asked whether sarcomeres undergo renewal through protein turnover. A pulse-chase approach was used to study the turnover of the fly Actin88F protein. Actin is the most abundant protein in muscle fibres [68] and the *act88F* gene was selected for this experiment because it is specifically restricted to the sarcomeres in IFMs [92]. To generate pulsed expression of a GFP-tagged Act88F (Act88F::GFP), or cytoplasmic eGFP control (eGFP), the TARGET system was used (Figure 2.2; Figure 3.2 A). Optimal labeling was obtained with a 28hr pulse of expression starting directly post-eclosion. This was sufficient to produce equivalent maxima of intensity to those observed when the pulse of expression was not followed by a chase but was not so long as to cause fluorescent saturation (see Materials and Methods). The localization of Act88F::GFP when expressed only in adults using the TARGET system was distinct to its localization when

Figure 3.2 Sarcomeric actin undergoes turnover in adult muscles

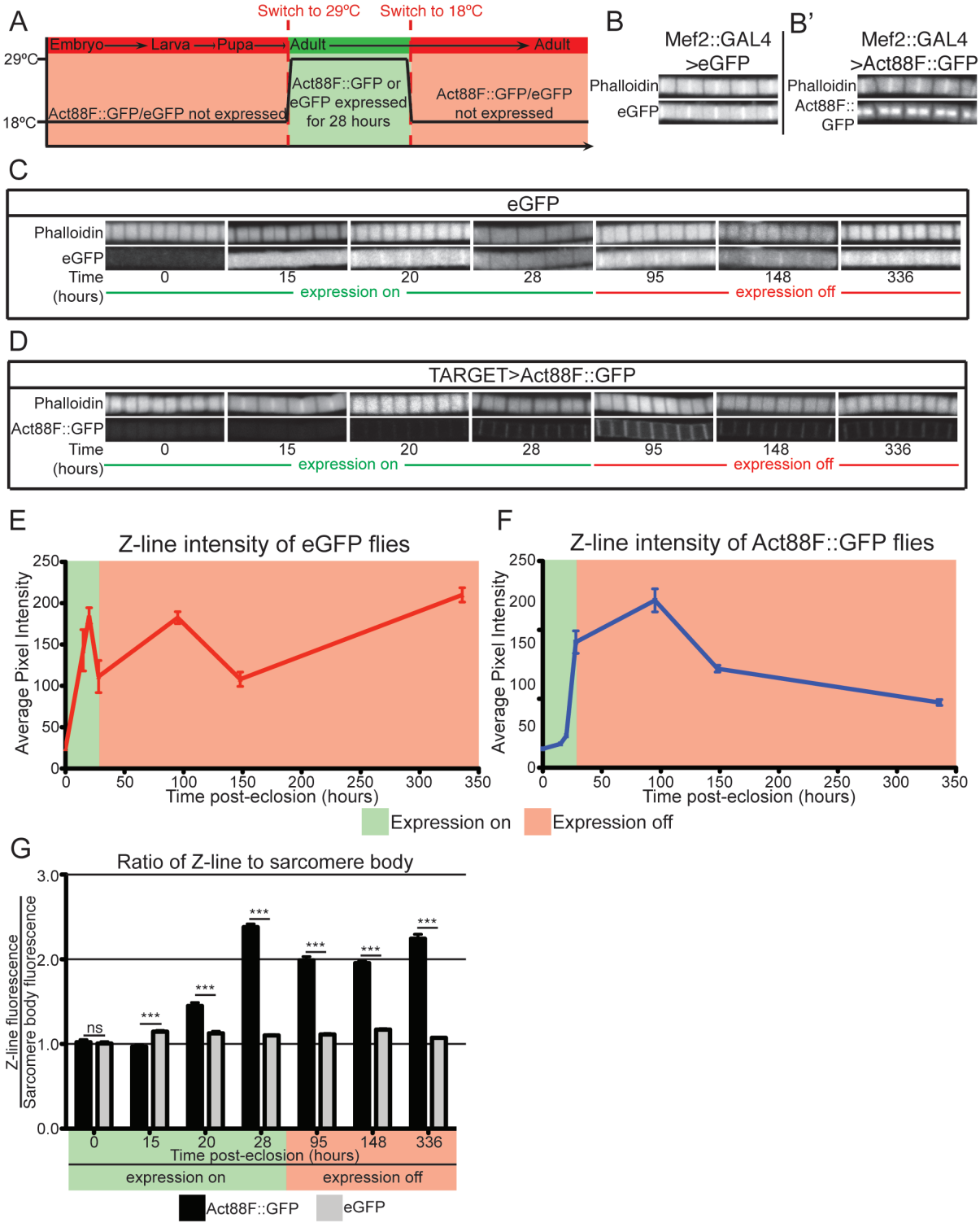

Figure 3.2 Sarcomeric actin undergoes turnover in adult muscles. (A) Experimental design for Act88F::GFP pulse-chase experiments. Act88F::GFP, or eGFP, was expressed under the control of the TARGET system. (B, B') Localization of eGFP (B) or Act88F::GFP (B') when expressed throughout life with the Mef2::GAL4 system (actin stained with rhodamine-phalloidin). eGFP labels the whole sarcomere while Act88F::GFP is only in the sarcomeric core. (C,D) A time series of representative images of IFMs from flies expressing eGFP (C) or Act88F::GFP (D) expressed under the TARGET system (stained with rhodamine-phalloidin). (E) Quantification of fluorescent intensity at the Z-disc for eGFP during TARGET pulse-chase experiment. Intensity at the Z-disc increased during the 28 hr pulse phase but did not decline afterwards. Instead, intensity remained elevated. (F) Quantification of fluorscent intensity at the Z-disc for Act88F::GFP during TARGET pulse-chase experiment. Intensity at the Z-disc increased during the 28 hr pulse phase and then gradually declines. (G) Calculating the ratio of Z-disc to sarcomere body staining intensity during pulse-chase experiment shows that the increase in staining intensity is specific to the Z-disc. Comparison of Z-disc to sarcomere body intensity ratios for eGFP (grey bars) and Act88F::GFP (black bars) expression. For (E,F,G) $N \geq 40$ individual sarcomeres from different muscles from multiple flies. For all panels, error bars indicate standard error; ns indicates not significant; * indicates a p-value<0.05, ** indicates a p-value<0.005, *** indicates a p-value<0.0005.

expressed throughout development by Mef2::GAL4 (compare Figure 3.2 B' and D). However, the localization of eGFP was similar under both conditions (compare Figure 3.2 B and C) which is consistent with non-specific incorporation of the eGFP.

By quantifying the fluorescence intensity at the Z-discs, I showed that Act88F::GFP was incorporated into the muscles beginning 20 hours after its expression was induced (Figure 3.2 D and F). After the expression of Act88F::GFP was repressed by shifting to the non-permissive temperature, intensity at the Z-disc continued to increase for 67 hours (Figure 3.2 D and F); subsequent to that point, intensity gradually decreased. At these later time points additional staining of Act88F::GFP was observed in the M-line and the muscle body, though this staining is substantially weaker than that observed in the Z-disc (Figure 3.2 D). In comparison, when a control pulse-chase experiment using a cytoplasmic eGFP showed that fluorescence became visible 15 hours after induction and that it remained at an elevated, fluctuating, level long after expression was repressed (Figure 3.2 E). My results suggest that the incorporation and turnover of Act88F::GFP was specific while that of eGFP was not.

I next demonstrated that the incorporation of Act88F::GFP was mostly restricted to the Z-disc using a quantitative image analysis approach. I calculated the ratio of fluorescent intensity at the Z-disc compared to the fluorescent intensity of the adjacent sarcomere body (see Materials and Methods). The ratio of Z-disc to sarcomere body intensity during expression of Act88F::GFP rose sharply, indicating that the Z-disc was the initial, and main, site for Act88F::GFP incorporation into the sarcomere (Figure 3.2 D and G). Once expression of the Act88F::GFP was repressed (chase-phase) the ratio decreased slightly although the majority of the Act88F::GFP continued to localize to the Z-disc (Figure 3.2 D and G). Comparatively, the ratio of Z-disc to sarcomere body intensity for eGFP expression showed a significantly lower Z-

disc localization at all time-points (Figure 3.2 C and G) although some Z-disc localization was evident (Figure 3.2 C). This data argues that the Z-disc is likely the major site of initial incorporation of newly synthesized Act88F::GFP in the adult muscle and that subsequently Act88F::GFP spreads into the rest of the sarcomere. Overall the pulse-chase experiments provide direct evidence that sarcomeric actin undergoes turnover in adult fly muscles and that actin is initially incorporated into the muscle at the Z-disc.

3.3 Designing a screen to identify genes required to maintain muscle function

The evidence thus far suggests that adult fly muscles undergo protein turnover at the sarcomere. Consequently, blocking the synthesis of specific proteins may have an adverse effect on muscle maintenance. In particular, I hypothesized that turnover of cytoskeletal proteins is important for muscle maintenance as the cytoskeleton forms the contractile machinery [11]. I tested my hypothesis directly by taking advantage of technical advances that make it possible to carry out a muscle specific gene knockdown screen in the adult muscles. The approach I used was an RNAi screen of candidate genes with a particular focus on cytoskeletal proteins. A library of RNAi lines was assembled that represented the fly cytoskeleton (see Materials and Methods) [87]. The cytoskeletal set was comprised of RNAi lines targeting 169 genes which represented actins and their associated proteins; tubulins and their associated proteins; motor proteins such as myosins, kinesins and dyneins; and other cytoskeletal elements including lamins, membrane linkers and septins. While I focused predominantly on cytoskeletal components (‘Cytoskeletal / Muscle’, 44 genes and ‘Cytoskeletal / Miscellaneous’, 125 genes; Figure 3.3 C) my screen also contained lines that targeted two other groups of interest: a set of non-cytoskeletal genes known to be essential for muscle function (‘Non-cytoskeletal/Muscle’; 29 genes), and a

Figure 3.3 An RNAi screen to identify genes required for muscle maintenance

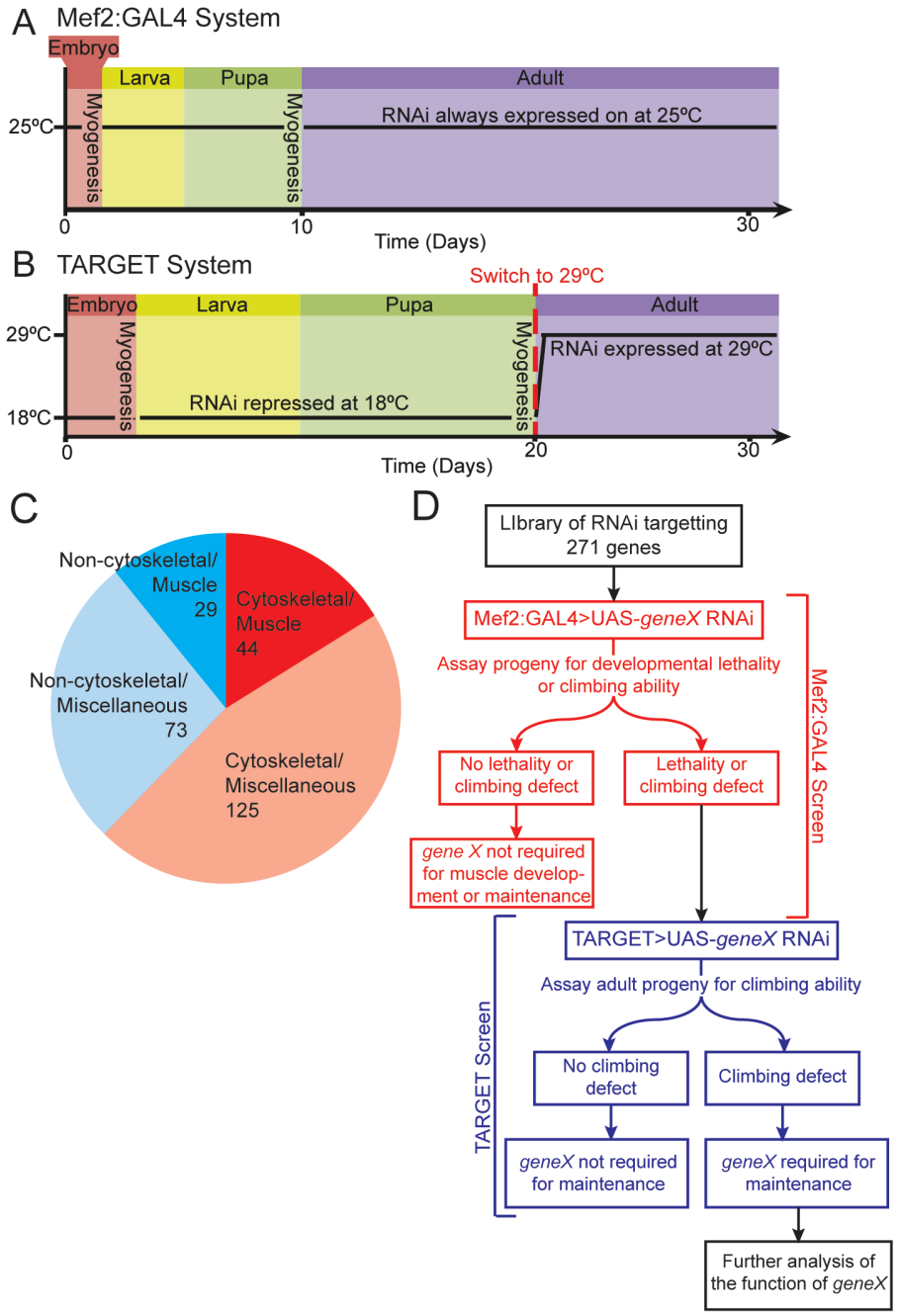

Figure 3.3 An RNAi screen to identify genes required for muscle maintenance. (A) The Mef2:GAL4 system. The Mef2:GAL4 system allows for muscle specific expression of RNAi using the GAL4/UAS system. (B) The TARGET system uses the Mef2:GAL4 system but includes a temperature-sensitive allele of the GAL4 repressor GAL80. At 18ºC, RNAi expression is turned off. At 29ºC, RNAi is expressed. To limit RNAi-mediated knockdown to adults, flies were kept at 18ºC until they eclosed, at which point they were transferred to 29ºC to induce RNAi expression. (C) A library of RNAi lines targeting 271 genes was assembled. Based on GO terms and literature searches, genes were classed into 4 catergories: 'Cytoskeletal/Muscle' (dark red, 44 genes); 'Cytoskeletal/Miscellaneous' (light red, 125 genes); 'Non-cytoskeletal/Muscle' (dark blue, 29 genes); and, 'Non-cytoskeletal/Miscellaneous' (light blue, 73 genes). (D) Flowchart of two-step screening protocol. In the first part of the screen, RNAi was expressed with the Mef2:GAL4 system. Lines that gave rise to phenotypes were then tested in the secondary screen using the TARGET system to assay for adult-specific defects.

control group of non-cytoskeletal genes that had no previously known function in muscle ('Non-cytoskeletal/Miscellaneous'; 73 genes) (Figure 3.3 C and Appendix C1). Classification was based on Gene Ontology annotations and the literature (see Materials and Methods). Although the library contained 271 genes, hits were retested using additional lines so in total 322 RNAi lines were screened during this work. Since the primary goal was to identify all the genes in the RNAi library that affected adult muscle function I designed a sensitive, comprehensive, and statistically robust functional screen. In the screen, an average of 50 flies (5 vials with 10 flies each) were screened for each line using a negative geotaxis (climbing) assay (see Materials and Methods). A key feature of the screen was its high time resolution that allowed me to detect subtle differences between control and knockdown conditions. A previous systematic RNAi knockdown screen in the fly assayed adult muscle function at a single time point 7 days post eclosion using a flight assay [63]. Assays were conducted every 3 days for the first 30 days of fly life; assays were stopped at 30 days because under screen conditions (29ºC) wild-type flies exhibited very low climbing ability at 30 days. The assay data was very statistically robust because of the large number of individual assays that went into screening each line. For example, each 30 day time course requires 275 individual assays: 5 vials were each assayed 5 times for each of the 11 time points. Representative examples that illustrate the effectiveness of such a sensitive screening approach are shown in Figure 3.6.

The screen was conducted in two phases. A primary screen where the RNAi was expressed using the Mef2::GAL4 driver [7] throughout life was designed to identify all the lines whose expression gave rise to phenotypes either during development or in the adult (see Materials and Methods; Figure 2.1; Figure 3.3 A and D). In the second phase all the lines whose knockdown in the muscle resulted in a phenotype were analyzed by expressing the RNAi only in

the adult muscle using the TARGET system. This part of the screen specifically identified lines required for muscle maintenance rather than muscle development (see Materials and Methods; Figure 2.2; Figure 3.3 B and D). In total, during the screening over 113,000 individual negative geotaxis assays were carried out.

3.4 Identification of cytoskeletal genes required for muscle function

The Mef2:GAL4 driver was used to express RNAi lines targeting the 271 candidate genes. Of these, 181 reached adult stage (Figure 3.4 A). The 90 genes whose knockdown resulted in lethal phenotypes were classified as either 'Embryonic lethal' (21 genes) or 'Pupal lethal' (69 genes); none showed larval lethality (Figure 3.4 A, Appendix C2). The 181 genes whose knockdown resulted in viable flies were studied using negative geotaxis assays and classified as those showing 'Adult climbing defect' (45 genes) or 'No defect' (136 genes) (Figure 3.4 A, Appendix C2). In total, the Mef2::GAL4 driven knockdown of 135 genes caused a phenotype suggesting that they are required for muscle function. For 45 of these genes, I repeated the RNAi knockdown with an alternate RNAi line that targeted a different part of the gene. 89% of these second lines also gave rise to a phenotype when expressed in muscle using Mef2::GAL4.

The distribution of Gene Ontology (GO) terms (www.geneontology.org) was analyzed in different phenotypic classes. An enrichment ratio was calculated that compared the prevalence of a certain GO term in a phenotypic class (eg: 'Embryonic lethal') to its prevalence in the entire screened library of genes (see Materials and Methods; Figure 3.4 C). Four broad GO-term based groupings were utilized: a 'Muscle' set with muscle related GO annotations, a 'Miscellaneous' set of genes with no muscle related GO annotation, a 'Cytoskeletal' set of genes, and a 'Non-

cytoskeletal' set (Figure 3.4 B). In general genes with cytoskeletal associated GO terms were enriched in the earlier, possibly more severe, phenotypic classes (Figure 3.4 B and C). However, there were some exceptions. For example hits in genes with microtubule-associated GO terms were rare (Figure 3.4 C). As muscle and cytoskeletal associated terms were likely to give earlier defects they were largely absent from the 'Adult climbing defect' class, exemplifying the need for using the TARGET system to analyze the function of such genes in later stages. Interestingly, the GO term 'Neuromuscular', while depleted in all other sets, was enriched in the 'Pupal Lethal' set (Figure 3.4 C). In general, within the set of all genes whose depletion resulted in a phenotype, a set I call 'All Hits', the only GO terms that showed enrichment were those integrally associated with muscle structures. This contrasts with a control group of genes classified with GO terms such as 'Intracellular', 'Extracellular', and 'Mitochondrion'. In this control group no enrichment or depletion of GO terms was observed in any of the phenotypic classes in the Mef2::GAL4 screen (Figure 3.4 C).

Figure 3.4 Results of the Mef2::GAL4 screen of the role of the cytoskeleton in muscle function

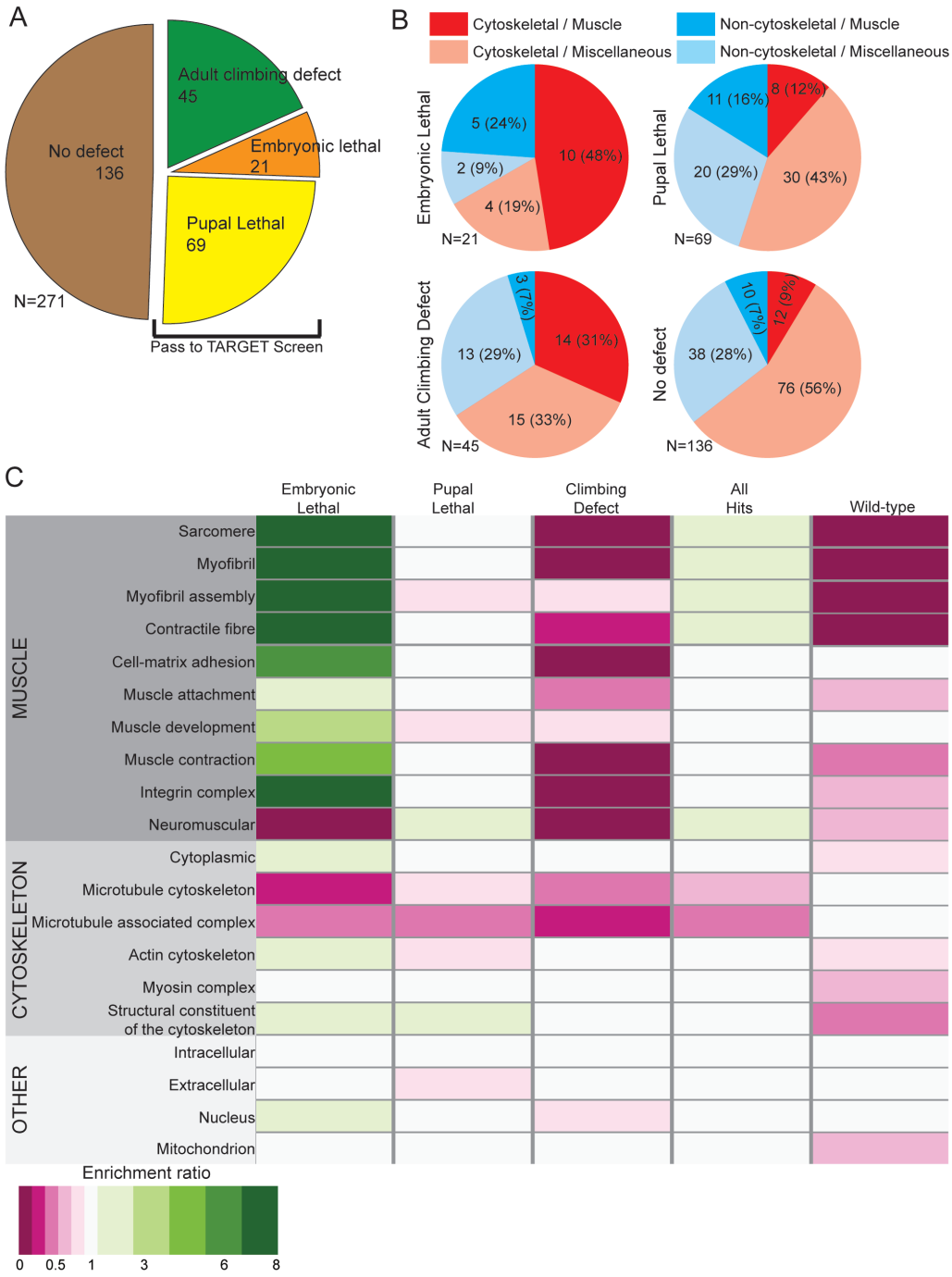

Figure 3.4 Results of the Mef2:GAL4 screen of the role of the cytoskeleton in muscle function. (A) Breakdown of phenotypes from Mef2:GAL4 system. 136 genes had no role in muscle development or maintenance (No defect, brown slice), 21 were Embryonic Lethal, 69 were Pupal Lethal, and 45 caused an Adult climbing defect. (B) Breakdown of each phenotypic class by general GO term. (C) Enrichment analysis of GO terms by phenotype. GO terms are listed on the left. Enrichment ratios were calculated by comparing frequency of a term in a specific phenotypic class to the frequency of the same term in the entire screened set. An enrichment ratio of 0 indicates that a given term did not appear in the phenotypic group. An enrichment ratio of <1 indicates that the frequency for the term was the reduced in the phenotypic class compared to the whole screened set. An enrichment ratio of 1 indicates that the frequency for the term was the same in the phenotypic class compared to the whole screened set. An enrichment ratio of >1 indicates that the frequency for the term was the enriched in the phenotypic class compared to the whole screened set.

3.5 Identification of genes specifically required for adult muscle maintenance

To identify genes specifically required for adult muscle maintenance, the TARGET system was used to limit RNAi expression to adults (Figure 2.2; Figure 3.3 B and D). The 135 genes identified in the Mef2::GAL4 screen whose knockdown resulted in phenotypes were screened in the TARGET screen (Figure 3.3 D). The TARGET screen identified 47 genes whose knockdown caused a significant decline in climbing ability in adult flies compared to wild type flies (Figure 3.5 A, Appendix C3), forty of which had no previously known role in muscle maintenance. The remaining 88 genes had no effect on adult climbing ability as assayed by the negative geotaxis assay (Figure 3.5 A, Appendix C3). Analysis of GO term distribution showed that muscle-associated terms such as myofibril assembly, sarcomere, muscle attachment, and cell-matrix adhesion were enriched in the 47 candidate genes (Figure 3.5 B and C). As a control, terms such as ‘Intracellular’, ‘Extracellular’, ‘Nucleus’, and ‘Mitochondrion’, showed no such enrichment.

Figure 3.5 Results of the TARGET screen for adult muscle maintenance

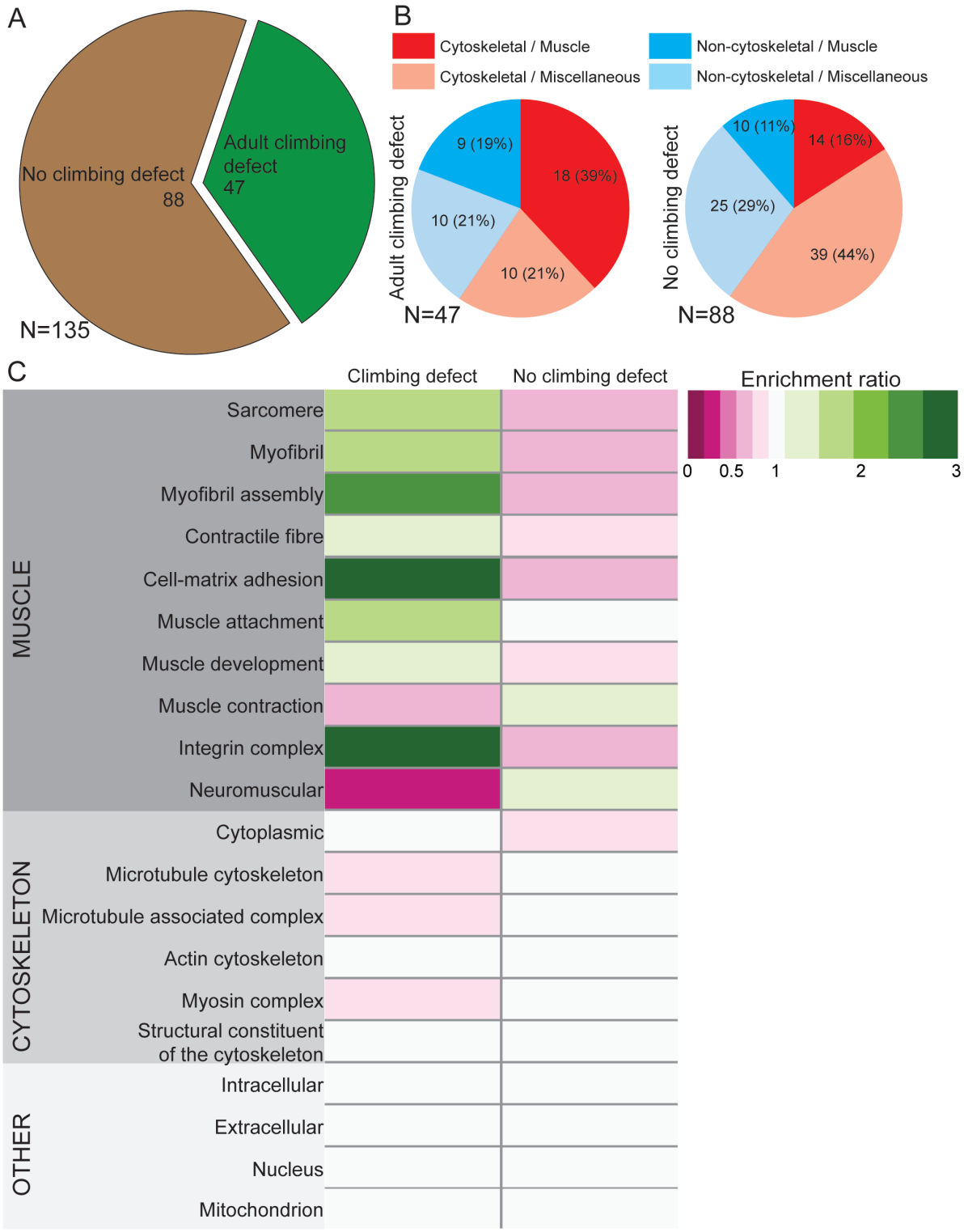

Figure 3.5 Results of the TARGET Screen for adult muscle maintenance. (A) Breakdown of phenotypes from the TARGET screen. 47 genes were identified as causing climbing defects in adults. (B) Breakdown of TARGET results by general gene function as defined by broad GO terms. (C) Enrichment analysis of GO terms by phenotype. GO terms are listed on the left. Enrichment ratios were calculated by comparing frequency of a term in a specific phenotypic class to the frequency of the same term in the entire screened set An enrichment ratio of 0 indicates that a given term did not appear in the phenotypic group. An enrichment ratio of <1 indicates that the frequency for the term was the reduced in the phenotypic class compared to the whole screened set. An enrichment ratio of 1 indicates that the frequency for the term was the same in the phenotypic class compared to the whole screened set. An enrichment ratio of >1 indicates that the frequency for the term was the enriched in the phenotypic class compared to the whole screened set.

3.6 Phenotypic classes identified in muscle maintenance screen

The severity of climbing defects caused by the gene knockdown varied widely; representative samples are shown in Figure 3.6. The phenotypes observed could be 'Severe', meaning complete loss of climbing ability within 9 days of RNAi induction (6 genes; Figure 3.6 A-C, Appendix C3), or 'Intermediate', meaning complete loss of climbing ability after 12 to 21 days of RNAi induction (13 genes; Figure 3.6 D-F, Appendix C3). However, the largest phenotypic category was the 'Weak' class, meaning complete loss of climbing ability did not appear until more than 24 days after RNAi induction (28 genes; Figure 3.6 G-I, Appendix C3). The remaining 88 genes, 'No defect', showed no difference from the control flies in climbing ability (Figure 3.6 J-L, Appendix C3). Overall, this screen identified a set of 47 genes whose ongoing synthesis is required for maintenance of adult muscle function.

Figure 3.6 Sample assay graphs from the TARGET screen

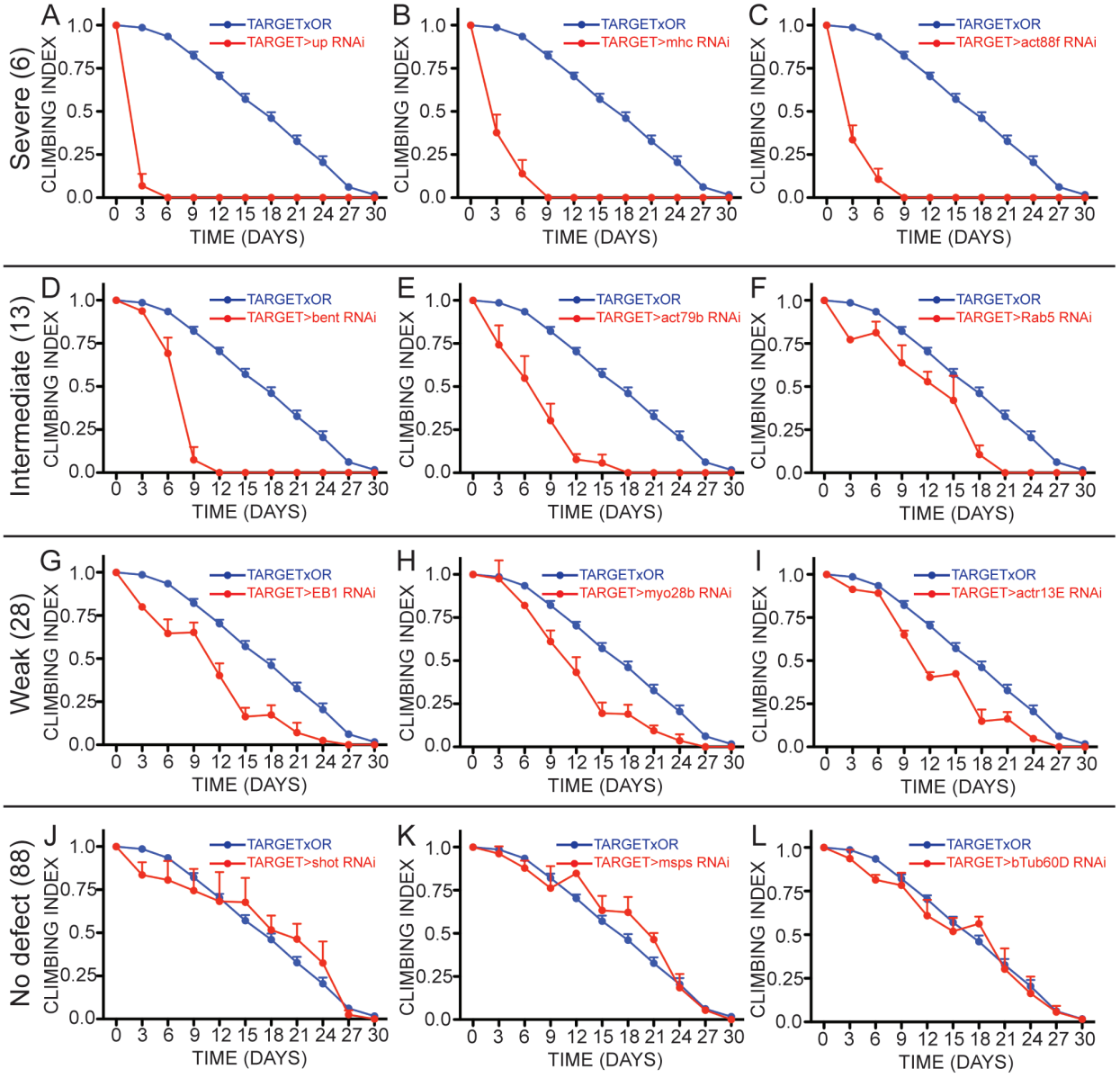

Figure 3.6 Sample assay graphs from TARGET screen. Severity of the climbing phenotype in the TARGET screen were ranked based on when flies lost the ability to climb. Loss of climbing ability between Day 0 and Day 9 were classed as 'Severe'; between Day 12 and Day 21 were classed as 'Intermediate'; between Day 24 and Day 30 as 'Weak'; and 'No defect' if climbing ability was not lost. (A-C) Examples of 'Severe' phenotypes. *up* RNAi (A), *mhc* RNAi (B), and *act88F* RNAi (C). In total, 6 genes had caused 'Severe' climbing defects. (D-F) Examples of 'Intermediate' phenotypes. *bent* RNAi (D), *act79B* RNAi (E) and *rab5* RNAi (F). In total, 13 genes caused 'Intermediate' phenotypes. (G-I) Example of 'Weak' phenotypes. *EB1* RNAi (G), *myo28B* RNAi (H) and *actr13E* RNAi (I). In total, 28 genes caused Weak' phenotypes. J-L. Examples of 'No defect' phenotypes. *shot* RNAi (J), *msps* RNAi (K) and *bTub60D* RNAi (L). In total, 88 genes caused 'No defect' to adult climbing ability. For all graphs, blue lines are the wild-type control and red lines are the RNAi knockdown line. Error bars are standard error.

3.7 Network analysis of genes identified in TARGET screen reveals key complexes in muscle maintenance.

To assemble a network of candidate hits from the screen a two-step approach was utilized. Firstly, the *Drosophila* Interactions Database (www.droidb.org) was used to identify genetic and biochemical interactions between the 47 genes shown in the TARGET screen to be required for muscle maintenance (Figure 3.7). Secondly, GO term analysis was used to group the 47 genes into broad functional categories in order to further arrange the interaction network (Figure 3.7). This approach highlighted the importance of the network of interacting sarcomeric protein in muscle maintenance (Figure 3.7). In particular, the key Z-disc component a-actinin (*actn*) appeared as an important link between the 'Sarcomeric' interaction cluster and other clusters in the network. One such cluster that links to α-actinin is the Integrin Adhesion Complex (IAC), which is important for muscle maintenance [75]. Interestingly, about a quarter of the genes identified in the TARGET screen are associated with the GO term 'Muscle Development', and over half of the genes in this category have not been previously assigned a role in muscle maintenance. Several signaling molecules were also in our list. Some, such as PKA-C1 and *sl* (PLC-g), interact with genes in the 'Cytoskeleton' and 'Muscle Development' clusters. Thus, my analysis identified key complexes of genes whose ongoing transcription and renewal is essential to maintain muscle function.

Figure 3.7 Genetic interaction network of TARGET screen hits.

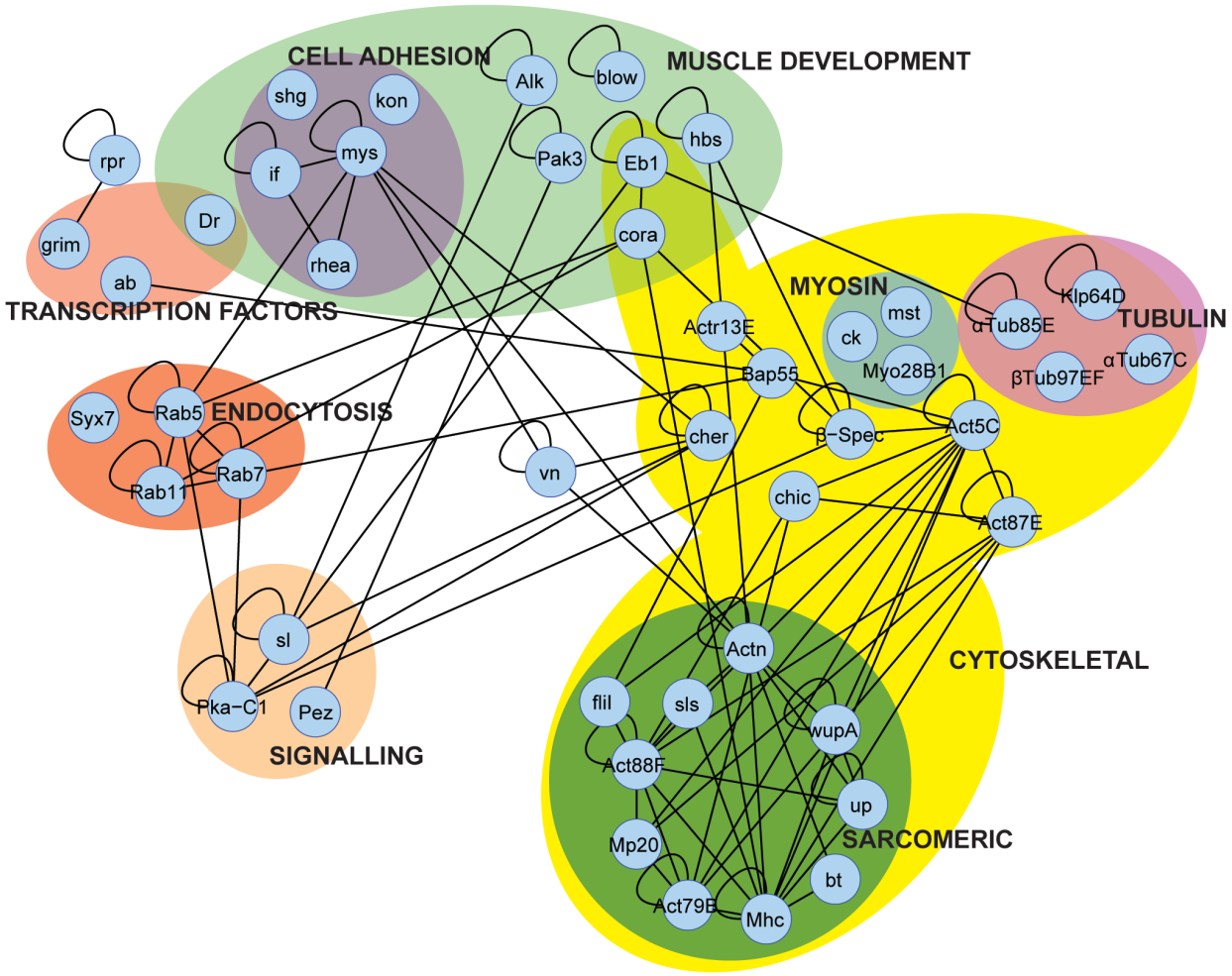

Figure 3.7 Genetic interaction network of TARGET screen hits. Genetic and biochemical interactions of the 47 genes identified in the TARGET screen were mined from the *Drosophila* Interactions Database (www.droidb.org). Using these interactions, the genes were then organized into groupings based on GO term analysis.

3.8 RNAi targeting *bent*, *mhc* or *act88F* causes significant reductions in mRNA levels

Based on the severity of the climbing defect caused by their knockdown (Figure 3.6), and their importance to sarcomeric structure, three genes were selected for further analysis: *bent*, *mhc*, and *act88F*. *bent* encodes the protein Projectin, which fulfills part of the Titin's role in the sarcomere and provides elasticity and structural support by linking thick filaments to the Z-disc [50]. *mhc* encodes Myosin Heavy Chain, which forms the thick filaments and binds to actin in a cyclical manner to generate contraction [11]. Finally, *act88F* encodes Actin88F, the IFM specific sarcomeric actin in the fly [11]. These three genes are, in general, the most abundant proteins in the sarcomere and loss of any of them during development causes defects in sarcomeric structure [12,50,68,70]. I confirmed, using qPCR, that the RNAi lines I used gave effective knockdown in the levels of all three genes (Figure 3.8 K-M). Although in wild-type flies there is a slight reduction in the level of these sarcomeric components over the first few days of life, the expression of the RNAi gave rise to significant depletion in mRNA levels compared to the wild-type (Figure 3.8 K-M). *bent* mRNA levels were reduced by 79% over 6 days of RNAi expression compared to a 30% reduction in control flies of the same age (Figure 3.8 K). *mhc* mRNA levels were reduced by 83% over 6 days of RNAi expression compared to a 36% reduction in control flies of the same age (Figure 3.8 L). *act88F* mRNA levels were reduced by 98% over 4 days of RNAi expression compared to only a 25% reduction in control flies of the same age (Figure 3.8 M). Since RNA was extracted from whole flies but the knockdown was carried out only in muscles these results may underestimate the extent of the knockdown and indicate that it is effective.

Figure 3.8 Loss of *act88F*, *mhc*, and *bent* does not disrupt sarcomeric architecture

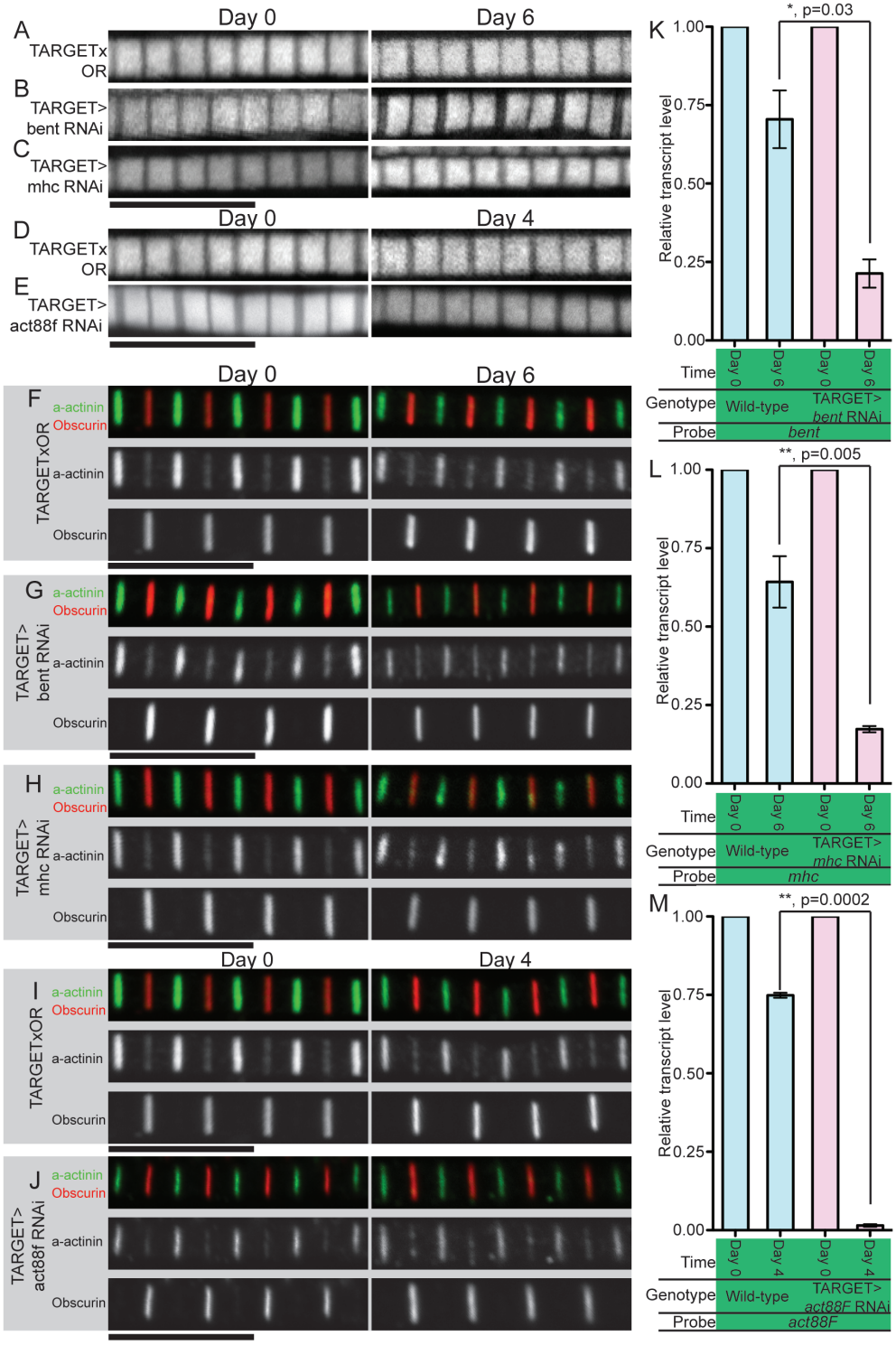

Figure 3.8 Loss of *act88F*, *mhc*, and *bent* does not disrupt sarcomeric architecture. Using phalloidin and antibody labelling, IFM integrity was examined before and after *bent*, *mhc* or *act88F* RNAi expression. For *bent* and *mhc*, RNAi was expressed for 6 days while for *act88F* RNAi was expressed for 4 days. (A-E). Phalloidin stainings of sarcomeric actin before and after RNAi expression showing no defects in actin filament organization after RNAi expression for all three genes. (F-J) Z-discs were labelled with an a-actinin antibody (green) and M-lines were labelled with an obscurin antibody (red). No disruption to the structural integrity of either structure was observed for all three genes. (K-M) qPCR analysis confirms that expression of RNAi transgenes targetting *bent*, *mhc* or *act88F* leads to substantial reduction in transcript levels for all three genes compared to control wild-type flies of equivalent age. For (K-M) $N \geq 2$ independent RNA extractions using >5 flies for each time-point were performed. For all panels, scale bars are 10 μm; error bars indicate standard error; ns indicates not significant; * indicates a p-value<0.05, ** indicates a p-value<0.005, *** indicates a p-value<0.0005.

3.9 Sarcomeric architecture is maintained after knockdown of *bent*, *mhc* or *act88F* in adult flies

To determine whether the climbing defects observed upon knockdown of *bent*, *mhc* and *act88F* were due to degeneration of the sarcomeres, sarcomeric architecture was analyzed using light microscopy and immunohistochemistry. IFMs were examined before and after RNAi induction. *bent* and *mhc* RNAi flies were imaged after 6 days while *act88F* RNAi flies were imaged after 4 days. The difference in timing was due to the severe effect of the RNAi knockdown on viability of *act88F* RNAi flies (Figure 3.6 B-D). Surprisingly, no obvious defects were observed in *bent*, *mhc* and *act88F* RNAi flies (Figure 3.8 A-E). The distribution and organization of actin as revealed by rhodamine-phalloidin staining appeared intact throughout in knockdown flies. Moreover, the integrity of the Z-disc and M-line was examined using antibodies to label the Z-disc (α-actinin [93]) and M-line (Obscurin [49]) (Figure 3.8 F-J). When *bent* and *mhc* RNAi flies were examined after 6 days of RNAi expression no defects were detected in either the Z-disc or M-line compared to the control flies (Figure 3.8 F-H). Similarly, no disruption to either the Z-disc or M-line was observed after 4 days of *act88F* RNAi expression (Figure 3.8 I and J). Taken together with the severe climbing defects observed for these three genes (Figure 3.6 B-D) the lack of obvious defects in actin organization in the sarcomere or Z-disc and M-line integrity suggests that sarcomeric structure may be disrupted in a subtler way. To address this possibility I used Transmission Electron Microscopy (TEM) to more closely study the ultrastructure of IFM sarcomeres (Figure 3.9). As before, *bent* and *mhc* RNAi was expressed for 6 days and *act88F* RNAi was expressed for 4 days. IFMs were imaged before and after RNAi expression. For all three genes no disruptions to Z-disc integrity (Longitudinal Sections) or filament lattice architecture (Transverse Sections) were observed (Figure 3.9 A-E).

Myosin filament-packing density is a useful measure of muscle organization and decline in density is associated with loss of muscle function [94]. In wild-type muscle, filament-packing density exhibits slight fluctuations over the first 6 days of adult life (Figure 3.1 C and E). Myosin filament packing density was quantified for *bent*, *mhc* and *act88F* RNAi flies (Figure 3.9 F-H). No significant difference in myosin filament packing density was observed after *bent*, *mhc*, and *act88F* knockdown (Figure 3.9 F-H). Therefore, despite the severe functional decline that occurs upon knockdown of *bent*, *mhc* and *act88F* I was unable to detect any disruptions to the overall integrity of the sarcomere.

Figure 3.9 Loss of *bent*, *mhc*, or *act88F* does not disrupt sarcomeric ultrastructure

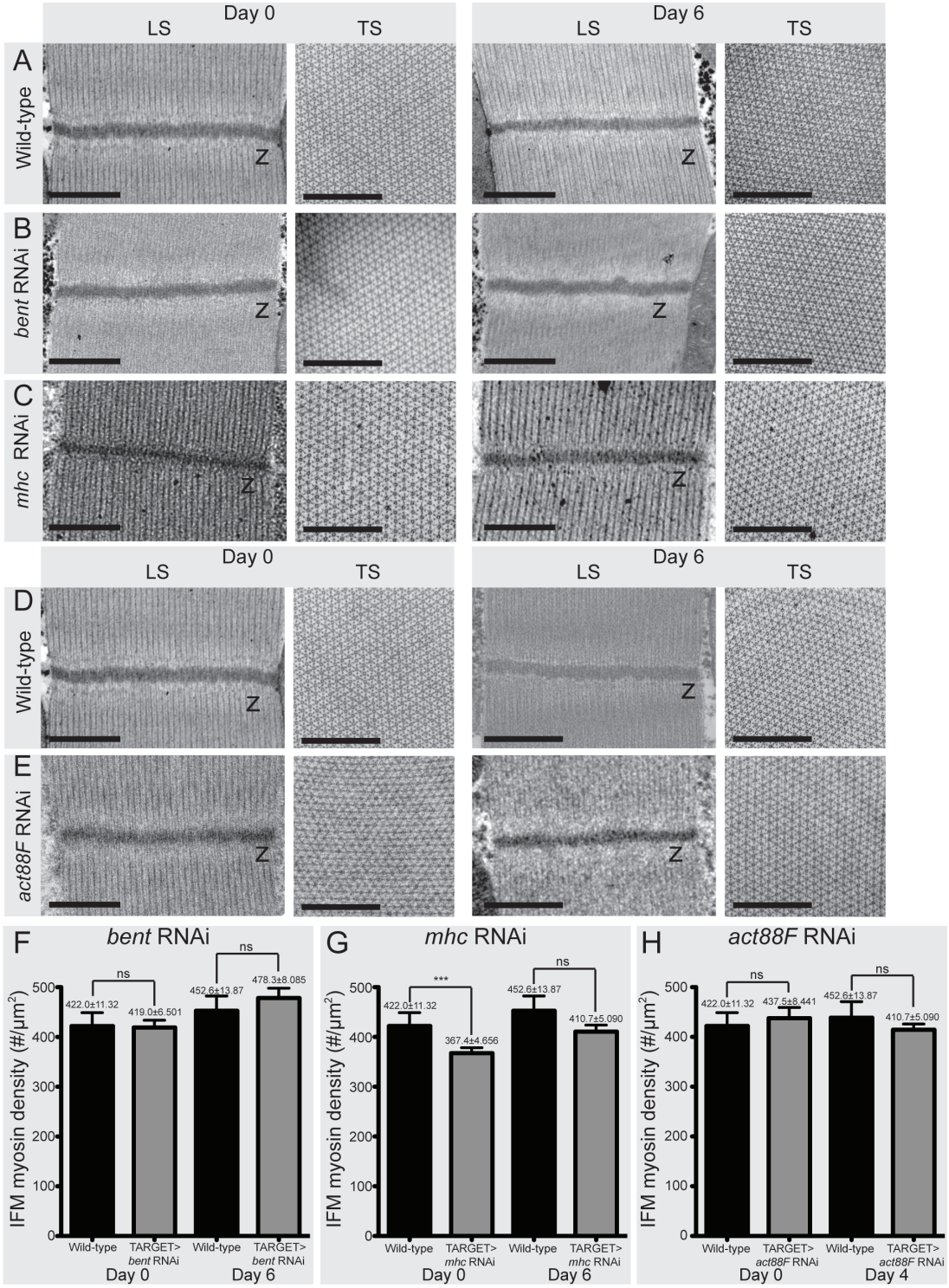

Figure 3.9 Loss of *bent*, *mhc* or *act88F* does not disrupt sarcomeric ultrastructure. Z-disc and thick and thin filament organization in *bent*, *mhc*, and *act88F* RNAi flies were examined using transmission electron microscopy. IFMs from *bent*, *mhc* and *act88F* knockdown flies were imaged before RNAi expression (Day 0) and after 6 days for *bent* and *mhc* and 4 days for *act88F*. (A-E) Electron micrographs of Longitudinal Sections and Transverse Sections of IFM sarcomeres before and after RNAi expression showing no defects in Z-disc integrity or myosin filament lattice architecture. (F-G) Quantification of myosin filament packing density in the *bent*, *mhc* and *act88F* knockdown flies showing no significant packing density differences after 6 days of RNAi expression, for *bent* and *mhc* RNAi, and 4 days of RNAi expression for *act88F* RNAi compared to wild-type control flies of equivalent age. For LS: 'z' indicates Z-discs; for TS: larger circles are myosin, smaller dots are actin. For all panels, scale bars are 500nm; error bars indicate standard error; ns indicates not significant; * indicates a p-value<0.05, ** indicates a p-value<0.005, *** indicates a p-value<0.0005. For (F-G) N≥3000 myosin filaments/time-point (>10 IFM transverse sections) from multiple flies.

3.10 *bent*, *mhc* and *act88F* are required to maintain sarcomere length in adult flies

Sarcomere length must be maintained due to key its key role in muscle function [95-97]. Therefore sarcomere length was examined in *bent*, *mhc* or *act88F* knockdown flies before and after RNAi induction using TEM. Sarcomere length was then measured Z-disc to Z-disc (see Materials and Methods). In wild-type muscles, sarcomere length shortened slightly with time, decreasing by 2.97% in first 6 days post eclosion (Figure 3.1 D, Figure 3.10 A and F). By comparison, in *bent* knockdown flies, greater shortening was observed with a decrease of 6.14% over the same time frame, meaning that after 6 days the bent sarcomeres were approximately 3% shorter than wild-type sarcomeres (Figure 3.10 A, B and F). Knockdown of *mhc* caused an even more pronounced sarcomere shortening, with a decrease of 13.8% over the same time frame, representing a 10% decrease relative to wild-type (Figure 3.10 A, C and F). Strikingly, the knockdown of *act88F* gave the opposite effect as sarcomere length increased by an average 13.53% (Figure 3.10 D, E and G). Overall, this data shows that knockdown of *bent*, *mhc* and *act88F* leads to defects in the maintenance of sarcomere length in the adult muscle.

Figure 3.10 *bent*, *mhc*, and *act88F* are required to maintain sarcomere length in flies

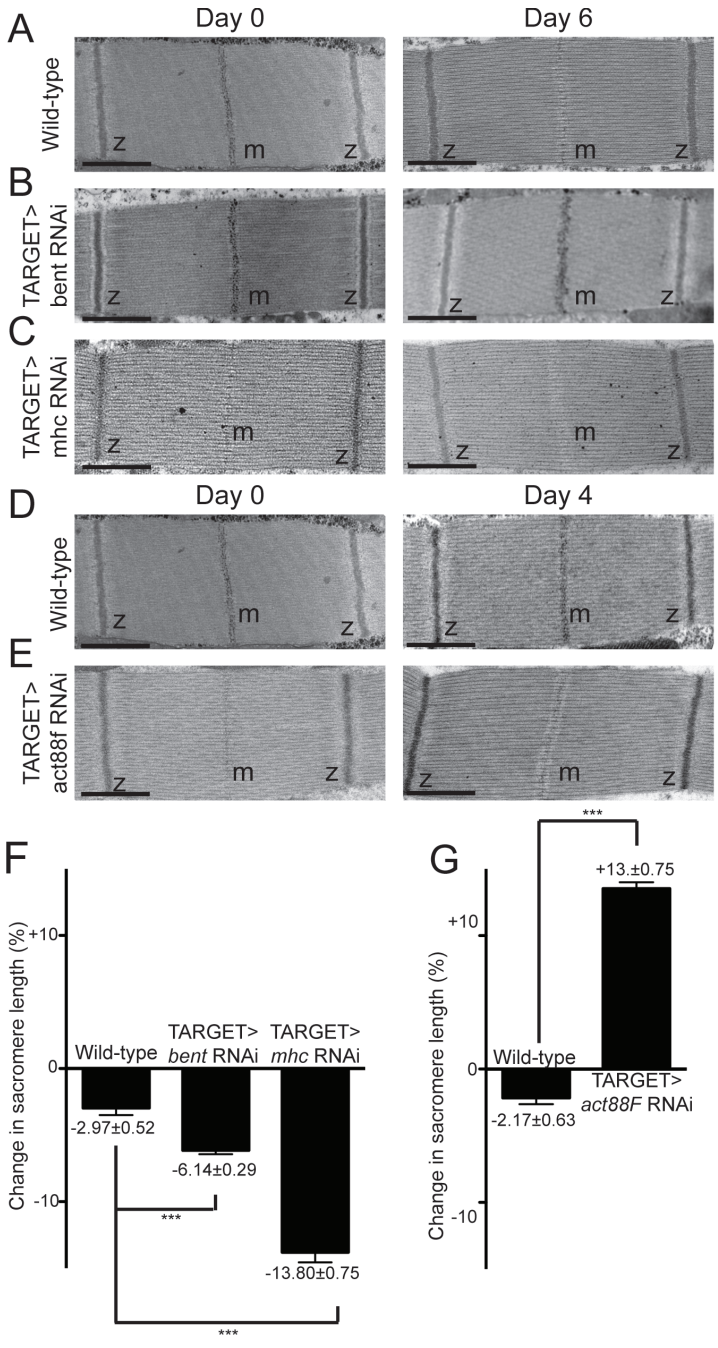

Figure 3.10 *bent*, *mhc* and *act88F* are required to maintain sarcomere length in adult flies. Sarcomere length was measured from electron micrographs to determine the effects of *bent*, *mhc* or *act88F* knockdown. Genotypes were fixed in parallel and length measurements were normalised to the Day 0 time point to allow calculation of the percent change in length. *bent* and *mhc* RNAi flies were imaged before RNAi expression (Day 0) and after 6 days of RNAi expression (Day 6), while act88F RNAi flies were imaged before RNAi expression (Day 0) and after 4 days (Day 4). (A-E) Transmission electron micrographs showing no ultrastructural defects. Close examination suggests changes in sarcomere length. (F-G) Length change as a percentage of intial length before RNAi induction for *bent* and *mhc* RNAi flies and control flies. Change in length is given as a percentage change from the length before RNAi induction (Day 0) to the length after RNAi induction (Day 6 for *mhc* and *bent*; Day 4 for *act88F*). (F) *bent* and *mhc* knockdown caused a decrease in sarcomere length compared to control flies. (G) *act88F* knockdown caused an increase in sarcomere length compared to the control flies. z, Z-disc. m, M-line; Scale bar = 1μm; For all panels, error bars indicate standard error; * indicates a p-value of less than 0.05, ** indicates a p-value of less than 0.005, *** indicates a p-value of less than 0.0005. For (F,G) N≥30 individual sarcomeres from different muscles from multiple flies.

3.11 Loss of *bent* does not disrupt thin filament length but reduces M-line width in IFM sarcomeres

Projectin (*bent*), and its partial functional vertebrate homolog Titin, is involved in regulating sarcomere length [43,98]. To more closely interrogate how *bent* knockdown effects sarcomere length, I analyzed the distribution of actin across the sarcomere by staining IFMs with phalloidin (Figure 3.11 A). Phalloidin labels sarcomeric actin (thin) filaments. As no filamentous actin is present in the M-line, this structure is evident by the absence of phalloidin staining. Measuring the pixel intensity of line across the phalloidin-labelled sarcomeres in a muscle fiber allows the determination of the thin filament length, M-line width, and overall sarcomere length (Figure 3.11 A and A'). This approach was used to analyze sarcomeres in *bent* knockdown flies before and after 6 days of RNAi induction. Sarcomere length was reduced in the *bent* RNAi flies but thin filament length was not disrupted relative to the wild-type (Figure 3.11 B-E). Moreover, the width of the M-line, interpreted as the distance between the two thin filament arrays, was significantly decreased in the *bent* knockdown flies (Figure 3.11 B, C and F). These results show that the overall disruption of sarcomere length observed upon *bent* RNAi knockdown in adult fly muscles is due to a reduction in M-line width and not the shortening of the thin filaments.

Figure 3.11 *bent* is required to maintain M-line width but not thin filament length in adult IFMs

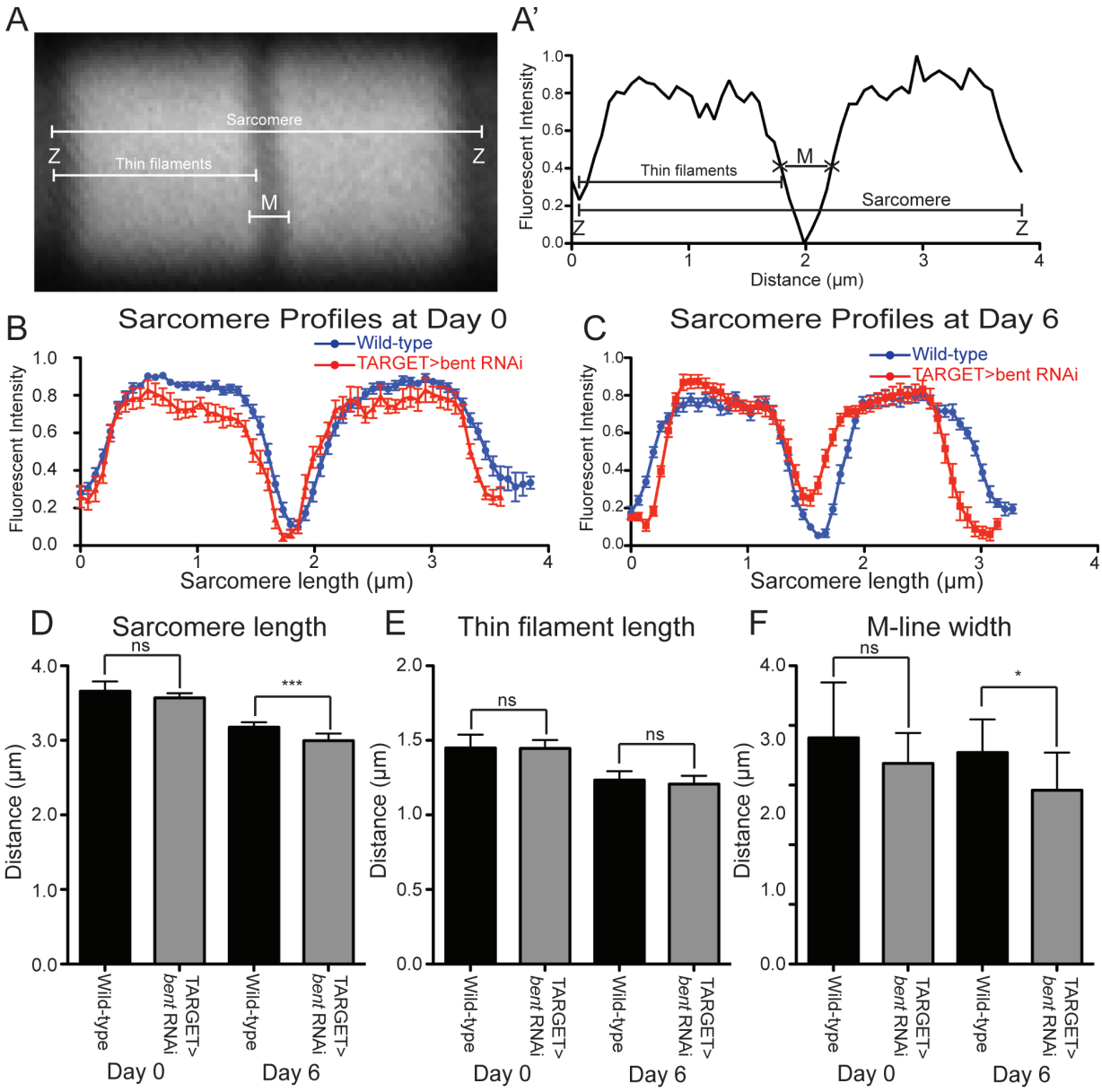

Figure 3.11 *bent* is required to maintain M-line width but not thin filament length in adult IFMs. Distribution of actin across the sarcomere was used to determine sarcomere length, thin filament length and M-line width. (A) Sample image of a single sarcomere labeled with phalloidin to show actin filaments. White overlay lines indicate quantified parameters. (A') Sample graph showing the intensity profile of a sarcomere representing the pixel intensities found along the overlay line labeled 'Sarcomere' in A. (B) Average intensity profiles across the sarcomere for *bent* RNAi (red line) and control flies (blue line) before RNAi induction. (C) Average intensity profiles across after six days of *bent* RNAi expression (red line) compared to control flies (blue line). (D) Quantification of sarcomere length from intensity profiles for *bent* RNAi flies before and after 6 days of RNAi expression compared to wild-type control flies of the same age. (E) Quantification of thin filament length from intensity profiles for *bent* RNAi flies before and after 6 days of RNAi expression compared to wild-type control flies of the same age. (F) Quantification of M-line width from intensity profiles for *bent* RNAi flies before and after 6 days of RNAi expression compared to wild-type control flies of the same age. For all panels, error bars indicate standard error; * indicates a p-value of less than 0.05, ** indicates a p-value of less than 0.005, *** indicates a p-value of less than 0.0005. For (B-F) $N \geq 15$ individual sarcomeres from different muscles from multiple flies for each time-point.

Chapter 4: Discussion and conclusion

4.1 Advantages and disadvantages of the screening methodology

Animal muscles are a remarkably robust tissue, maintaining their structure and function through ongoing cycles of contraction and relaxation. It is their ability to carry out this function reliably and consistently that underlies animal locomotion. However, we presently know little about the mechanisms that facilitate their ability to maintain their function over the life of an organism. I have gained insight into this process through a genetic screen designed to take advantage of the amenability of fly muscles to large-scale genetic analysis. Previous large-scale screens, both *in vivo* and in primary cell culture, have established the fly as an excellent system in which to analyze muscle function [63] as well as specific aspects of muscle development such as myoblast fusion [99], myotube targeting [100], and muscle assembly [101]. Unlike these other screens, this screen focused on the adult fly by limiting both gene knockdown and functional assays to flies that had completed myogenesis. The advantage of such an approach is that I can specifically identify those genes that are required for ongoing muscle function using a statistically robust approach. The disadvantage of such an approach is that it is labour-intensive and time-consuming and for this reason the screen was limited to a list of 271 candidate genes. By combining the tools of genomics with a more targeted approach I identified a good number of candidate genes (47 out of 271 or 17.3%) most of which had not been previously assigned a role in muscle maintenance. Importantly, only one of the genes identified in the screen was also identified in the very comprehensive genome-wide screen [63] as being required for muscle function in the adult, illustrating the usefulness and novelty of my approach.

4.2 Adult muscles are a dynamic tissue

As a complimentary approach to the identification of genes whose knockdown in the adult results in failure to maintain muscle function I characterized, in the adult fly, the transcription of sarcomeric components as well as the turnover of sarcomeric actin. It has long been known that muscles are highly dynamic when they undergo cell fusion, migration, cellular rearrangement, and assemble the cytoskeletal machinery of the sarcomere during myogenesis. I now show that they are in fact dynamic throughout adulthood. Furthermore, I demonstrate that sarcomeric actin undergoes protein turnover in the adult sarcomere, primarily at the Z-disc. Combining the previous results with those of my screen, it is clear that adult muscle is always in a state of flux and renewal. Moreover, this thesis shows that turnover of a key subset of cytoskeletal proteins underlie long-term muscle maintenance.

4.2.1 Adult IFMs show subtle changes to morphology over time

The muscle architecture, in particular the cytoskeletal architecture, becomes disorganized in aged flies (~50 days or older) [91]. However, it was not previously known whether, and to what extent, muscles in younger flies, and in particular during the first few weeks of life, also change with time. I showed that during this early stage of muscle life, no degeneration occurs to sarcomere ultrastructure. However, subtle changes to both sarcomere length and myosin filament density were observed during this time, indicating that muscle tissue is dynamic. Sarcomere length has been observed to fluctuate in developing, larval *Drosophila* muscles [102], flies mutant for key sarcomeric proteins [73] and during metamorphosis [103]. Furthermore, myosin packing density is disrupted in Mhc mutants [70]. However, this work represents the first time that such changes have been observed as a function of time in wild-type animals.

4.2.2 New proteins are continually synthesized and incorporated into adult IFMs

In this thesis, I have shown that over the first 30 days of fly life muscles, key sarcomeric genes are continually transcribed. This result is consistent with previous work showing that sarcomeric components were expressed in adult fly muscles [104]. As such I hypothesized that the protein products of this gene transcription would be involved in protein turnover in adult muscles. To test this, I expressed a GFP-labeled Act88F transgene in adult muscles. As hypothesized, I saw Z-disc specific incorporation of the Act88F::GFP. This data is in line with body of literature illustrating protein turnover in sarcomeres of cultured mouse myocytes [105], cultured chick cardiac and rat skeletal muscles [81,106], and the body wall muscles of adult nematodes [107]. Nonetheless, my study is unique because it follows the turnover of sarcomeric actin over many days in intact animals and at multiple time points. In particular, my analysis reveals that sarcomeric actin is rapidly incorporated into the muscle and remains there for a period of days. Moreover, I observed that the majority of the actin incorporates in the sarcomere at the Z-disc. This finding is in line with previous results suggesting that the Z-disc is a dynamic structure [13,108] as well as with the hypothesis that the Z-disc serves as the initial point of actin incorporation into sarcomeres[43]. The notion that the Z-disc acts as a site for actin incorporation into the sarcomere is particularly appealing as the barbed-end of sarcomeric actin filaments are located in the Z-disc and actin monomers are added to the barbed-end during polymerization [98]. It should be noted that out results indicate that the turnover rate of actin in adult muscle sarcomeres is in line with that observed in cultured muscles. The *in vivo* analysis of actin turnover rates showed that turnover occurred over many hours or days, a result consistent with studies in rat and mouse myocytes [81,105]. In summary, I demonstrated that synthesis and turnover of core sarcomeric proteins is a feature of adult fly muscles and that the Z-disc is the

initial point of incorporation for new actin.

4.3 Careful analysis of muscle function reveals many candidate genes required for muscle maintenance

Based on the results that reveal the adult muscle as a dynamic system it is perhaps not surprising that I identify many genes whose ongoing expression is required to maintain muscle function. Nonetheless, a key aspect of my screen was the high-resolution, statistically-robust assays I performed. Had I assayed muscle function only once, a week after flies had eclosed, as had been previously done [63], rather than every 3 days and in quintuplicate, I would have missed a substantial number of candidate hits. In this respect this screen represents a compromise between genome wide low-resolution/high-throughput studies and high-resolution/low-throughput analyses of single genes. Moreover, this high-resolution approach is necessitated by the observation that wild-type flies exhibit a natural decline in muscle function over the first thirty days of life immediately following eclosion [41,75,109]. This meant that that in effect I was screening for genes that enhanced a decline that already exists in the wild-type, a somewhat subtle phenotype. It is unclear what causes this decline in wild-type flies, but it is likely related to behavioral and environmental changes [110]. To account for this decline, I modified the design of my screen was accordingly by comparing the climbing ability of RNAi knockdown flies to the wild-type at each assayed time point.

4.3.1 The Mef2::GAL4 screen reveals key functional classes of genes required for muscle development

The initial screen, using Mef2::GAL4 which is expressed throughout muscle development, was designed to identify RNAi lines whose expression gives rise to phenotypes during muscle development. Furthermore, it allowed us to draw a number of useful additional conclusions. Firstly, 89% of the genes I screened in the Mef2::GAL4 screen were previously screened in the genome wide RNAi screen [63]; of these, the expression of RNAi targeting 82% gave rise to the same phenotypes in both screens, a high degree of overlap that validates both screens. Secondly, compared to a control group of miscellaneous genes I observed a higher hit rate for the group composed of genes that are classified under GO terms in the cytoskeletal and muscle category. Unsurprisingly, I saw strong enrichment in the list of candidate genes for GO terms in myofibril structure and development category, especially in the more severe lethal phenotypic group. This underscores the importance of screening such genes by limiting RNAi knockdown in the adult, as I did in the TARGET screen. Finally, although GO terms for actin, myosin, and their respective binding partners were enriched in the Mef2:GAL4 screen, genes annotated with microtubule-associated GO terms were largely absent from the list of candidates for all phenotypic groups. This may suggest that microtubule dynamics serve a more restricted role in muscle development, or that a small core of microtubule-associated proteins mediates such roles. In summary, these results highlight the importance of the actin and myosin cytoskeleton in the initial round of myogenesis.

4.3.2 The TARGET screen identified 47 genes required to maintain adult muscle function

The two-step screening protocol enabled us to eliminate half of the total set of genes from the more labor-intensive TARGET screen. Of the 135 genes I screened using the TARGET system only 47 (35%) were identified as being required for adult muscle maintenance though all gave phenotypes when knocked-down throughout muscle development with Mef2::GAL4. This suggests that fewer genes are required for maintaining muscles than are required for building muscles. Interestingly, 22 genes that gave an adult climbing defect when knocked down with Mef2::GAL4 did not do so with the TARGET system suggesting that the adult phenotypes are a result of abnormal muscle development and supporting the assertion the genes identified in the TARGET represent a unique set. GO term analysis of the candidates identified in the TARGET screen provided some intriguing insights into the comparative roles of genes in muscle development and maintenance. Unsurprisingly, genes annotated with myofibrillar GO terms were enriched in the set of genes that are required for muscle maintenance as were components of the integrin adhesion complex, which is consistent with my previous results [75]. There is therefore substantial overlap in the set of genes that make muscle and those that maintain it. Moreover, network analysis of the candidate genes reveals clusters of interacting genes, likely complexes, which are important for maintaining muscle function. While the most prominent of those is, as expected, the sarcomeric cluster of proteins, a number of other clusters are identifiable including the endosomal cluster of Rab11/Rab5/Rab7. Importantly the network analysis helps identify genes that serve an important function in linking different clusters, most prominently the genes *actn* (α-actinin) and *cora* (coracle).

4.4 Core sarcomeric genes are not required to maintain sarcomeric integrity

Although the screening methodology was designed to identify subtle phenotypes it is still surprising that knockdown of the candidate sarcomeric genes *bent*, *mhc* and *act88F*, which all caused robust functional defects, did produce more substantial defects in terms of disrupting muscle architecture and morphology. This finding suggests that in adult flies it is possible to obtain a large functional defect prior to the appearance of substantial morphological defects. As muscles are a delicately balanced system in which structure and function are so closely linked [111], it is possible that perturbations to their structure that do not cause noticeable defects result in severe functional defects. There are several other possibilities to explain the lack of a morphological defect to sarcomere architecture or ultrastructure. A subset of the candidate genes may affect neuronal function, potentially by having an essential role in the NMJ; such candidates include *abrupt* and the Rab genes [112-115]. Another possibility is that the decline in climbing ability is due to muscle-type specific phenotypes such as defects in the fly heart muscle rather than a general defect in muscle maintenance. However it is unlikely that core sarcomeric components such as actin, Projectin, and Mhc are required specifically in some muscle-types more than others. Finally, one common pathway implicated in loss of muscle function in adult flies is mitochondrial degeneration [53,54]. RNAi is an effective method of inhibiting mitochondrial genes in Drosophila [116-118]. However, mitochondrial GO terms show no enrichment in the set of candidate genes suggesting that loss of mitochondrial function does not play a large role in the functional phenotypes observed in the screen. Nonetheless, I suspect that failure to maintain proper sarcomere integrity underlies the functional phenotypes observed in at least some of the 44 other candidate genes although there are other alternatives.

4.4.1 Careful analysis of sarcomeric dimensions reveals defects in sarcomere length

Although no defects were observed to the sarcomeric architecture or ultrastructure, when 3 candidate genes were chosen and analyzed in greater detail a notable morphological defect was identified, namely a disruption in sarcomere length. Interestingly, I observed opposite effects in the 3 candidate genes examined. While *bent* and *mhc* knockdown caused shortened sarcomeres, *act88F* knockdown caused an increase in sarcomere length. These differences might be due to the different roles of thin filament (actin) and thick filament (Mhc, Projectin) proteins play in maintaining proper sarcomere dimensions. It is important to note that the observed defects in sarcomere length lie are larger than the slight changes observed during IFM contraction [47]. My working hypothesis, that the observed functional defects induced by the knockdown of the candidate genes are caused by changes in sarcomere length, is in line with previous observations in the literature [61,96,103]. It is, for example, known that mutations in sarcomeric components such as Mhc and Troponin-T screen lead to changes in sarcomere length by causing muscle hypercontraction [73]. It should be noted that although the phenotypes I observe in *bent* and *mhc* knockdown flies are reminiscent of muscle hypercontraction mutants they differ somewhat. Hypercontraction typically refers to excessive contraction or underlying developmental defects that disrupt the regulation of contraction in adult flies [70,73]. As defined previously [73] sarcomere shortening, and hypercontraction in particular, is associated with filament density disruption and other ultrastructural defects which I do not observe. I predict that further analysis of the 47 candidate genes I identified will reveal there is no universal underlying mechanism for muscle maintenance. However, knockdown of Mhc, Projectin, or actin in the adult muscle caused disrupted sarcomere length suggesting that the ongoing synthesis and turnover of core components of the sarcomere is important for maintaining sarcomere length.

4.5 Loss of *bent* disrupts maintenance of M-line width

The abnormal M-line phenotype I observe upon knockdown of *bent* (Projectin), a partial functional ortholog of Titin, is in line with studies that implicated vertebrate Titin in maintaining sarcomeric architecture and in particular M-line integrity [119]. I used two different methods, based on light and electron microscopy, to characterize the dimensions of the sarcomere and its various parts in *bent* knockdown flies and found a reproducible reduction in sarcomere length. Although such disruptions to sarcomere length typically result from decreased thin filament length which is characteristic of a variety of myopathies [98], I observed no change in thin filament length in *bent* knockdown flies. However, I observed that the width of the M-line decreases in *bent* RNAi flies compared to wild-type flies. Disruption of M-line integrity causes a functional decline in muscles [120]. My data suggests that knockdown of *bent* leads to a disruption of sarcomere length through a narrowing of the M-line. Several possible mechanisms exist for the observed reduction in M-line width. Titin/Projectin have been proposed to be involved in maintaining sarcomere length by acting as a sarcomeric ruler [43,98]. Given the known role of Titin/Projectin as a scaffold that links the Z-disc and the thick filaments I speculate that a reduction in Projectin levels could result in disruption of the linkage between the thick filament and the Z-disc [121]. Consequently, failure to maintain proper attachment between the Z-disc and the thick filament could lead to a collapse of the sarcomere upon itself, a similar state to that which exists in a contracted muscle, and this would result in narrowing of the M-line. Nonetheless, there are alternative models. For example, it has been proposed that sarcomere shortening could act as a protective adaptation in weakened muscles as shorter sarcomeres generate less force [61,122]. Such an adaptation has been proposed in the context of M-line disruption for Sarcoglycan mutant flies [61]. In general, my data underscores the importance of

maintaining proper sarcomere dimensions throughout the life of the organism and highlight the role of protein turnover in this process.

4.6 Conclusions

The data presented in this thesis show that the ongoing synthesis and turnover of a subset of muscle proteins is essential for maintaining muscle function. Moreover, the Z-disc was identified as the initial site of protein turnover within the sarcomere. I propose, based on my observation of actin dynamics over multiple days in adult muscle, that the Z-disc provides an entry point for newly synthesized proteins, which then spread throughout the rest of the sarcomere. Failure to renew muscles through protein turnover results in accelerated functional decline compared to wild-type flies; since muscles experience continual stress this may be due a failure to replace proteins that have been damaged by mechanical forces, which then accumulate and impinge on muscle function. This could explain why I did not see stronger ultrastructural defects when knockdown flies were examined; proteins might be present, preserving the ultrastructure, but their function could be compromised due to mechanical or oxidative damage. Consistent with this idea, the defects that were observed in M-line integrity and sarcomere length are reminiscent of, though not identical to, other conditions that involve altered mechanical force in the muscle, such as hypercontraction and M-line disorganization [61,73,96]. In addition it is intriguing to speculate that this screen provides a model for some of the functional decline associated with the process of aging. I hypothesize that aging-associated functional decline is due to a reduced ability of the muscle to replace damaged components. In line with this hypothesis studies on aging muscle in flies and humans show that aging is associated with a general decrease in the synthesis of proteins in the muscle [91,123]. The genes I identified in this screen

represent excellent candidates to study in the context of myopathy and aging. Furthermore, they are potential therapeutic targets in the treatment of myopathies characterized by accelerated, aging-associated loss of adult muscle function.

Bibliography

1. Clark KA, McElhinny AS, Beckerle MC, Gregorio CC (2002) Striated muscle cytoarchitecture: an intricate web of form and function. Annu Rev Cell Dev Biol 18: 637-706.

2. Bergmann O, Bhardwaj RD, Bernard S, Zdunek S, Barnabe-Heider F, et al. (2009) Evidence for cardiomyocyte renewal in humans. Science 324: 98-102.

3. Augustin H, Partridge L (2009) Invertebrate models of age-related muscle degeneration. Biochim Biophys Acta 1790: 1084-1094.

4. Dietzl G, Chen D, Schnorrer F, Su KC, Barinova Y, et al. (2007) A genome-wide transgenic RNAi library for conditional gene inactivation in Drosophila. Nature 448: 151-156.

5. McGuire SE, Le PT, Osborn AJ, Matsumoto K, Davis RL (2003) Spatiotemporal rescue of memory dysfunction in Drosophila. Science 302: 1765-1768.

6. Ni JQ, Liu LP, Binari R, Hardy R, Shim HS, et al. (2009) A Drosophila resource of transgenic RNAi lines for neurogenetics. Genetics 182: 1089-1100.

7. Ranganayakulu G, Elliott DA, Harvey RP, Olson EN (1998) Divergent roles for NK-2 class homeobox genes in cardiogenesis in flies and mice. Development 125: 3037-3048.

8. OOta S, Saitou N (1999) Phylogenetic relationship of muscle tissues deduced from superimposition of gene trees. Mol Biol Evol 16: 856-867.

9. Fitts RH (1994) Cellular mechanisms of muscle fatigue. Physiol Rev 74: 49-94.

10. Schnorrer F, Dickson BJ (2004) Muscle building; mechanisms of myotube guidance and attachment site selection. Dev Cell 7: 9-20.

11. Vigoreaux JO (2006) Molecular basis of muscle structure. In: Sink H, editor. Muscle Development in Drosophila. New York/Georgetown: Springer/Landes Bioscience. pp. pp 143-156.

12. Rui Y, Bai J, Perrimon N (2010) Sarcomere formation occurs by the assembly of multiple latent protein complexes. PLoS Genet 6: e1001208.

13. Sanger JW, Wang J, Fan Y, White J, Sanger JM (2010) Assembly and dynamics of myofibrils. J Biomed Biotechnol 2010: 858606.

14. Bullard B, Garcia T, Benes V, Leake MC, Linke WA, et al. (2006) The molecular elasticity of the insect flight muscle proteins projectin and kettin. Proc Natl Acad Sci U S A 103: 4451-4456.

15. Linke WA, Ivemeyer M, Mundel P, Stockmeier MR, Kolmerer B (1998) Nature of PEVK-titin elasticity in skeletal muscle. Proc Natl Acad Sci U S A 95: 8052-8057.

16. Wang K, McClure J, Tu A (1979) Titin: major myofibrillar components of striated muscle. Proc Natl Acad Sci U S A 76: 3698-3702.

17. Littlefield R, Almenar-Queralt A, Fowler VM (2001) Actin dynamics at pointed ends regulates thin filament length in striated muscle. Nat Cell Biol 3: 544-551.

18. Littlefield RS, Fowler VM (2008) Thin filament length regulation in striated muscle sarcomeres: pointed-end dynamics go beyond a nebulin ruler. Semin Cell Dev Biol 19: 511-519.

19. Farah CS, Reinach FC (1995) The troponin complex and regulation of muscle contraction. FASEB J 9: 755-767.
20. Gunning P, O'Neill G, Hardeman E (2008) Tropomyosin-based regulation of the actin cytoskeleton in time and space. Physiol Rev 88: 1-35.
21. Ervasti JM (2003) Costameres: the Achilles' heel of Herculean muscle. J Biol Chem 278: 13591-13594.
22. Linnemann A, van der Ven PF, Vakeel P, Albinus B, Simonis D, et al. (2010) The sarcomeric Z-disc component myopodin is a multiadapter protein that interacts with filamin and alpha-actinin. Eur J Cell Biol 89: 681-692.
23. Meissner B, Warner A, Wong K, Dube N, Lorch A, et al. (2009) An integrated strategy to study muscle development and myofilament structure in Caenorhabditis elegans. PLoS Genet 5: e1000537.
24. Ciena AP, Luques IU, Dias FJ, Yokomizo de Almeida SR, Iyomasa MM, et al. (2010) Ultrastructure of the myotendinous junction of the medial pterygoid muscle of adult and aged Wistar rats. Micron 41: 1011-1014.
25. James Darnell (1990) Muscle Structure and Function. In: Darnell JE, editor. Molecular Cell Biology. 2nd ed. Baltimore, USA: Scientific American Books. pp. 865-879.
26. Herrmann H, Strelkov SV (2011) History and phylogeny of intermediate filaments: now in insects. BMC Biol 9: 16.
27. Figeac N, Daczewska M, Marcelle C, Jagla K (2007) Muscle stem cells and model systems for their investigation. Dev Dyn 236: 3332-3342.
28. Richardson BE, Nowak SJ, Baylies MK (2008) Myoblast fusion in fly and vertebrates: new genes, new processes and new perspectives. Traffic 9: 1050-1059.
29. Sparrow JC, Schock F (2009) The initial steps of myofibril assembly: integrins pave the way. Nat Rev Mol Cell Biol 10: 293-298.
30. Bate M (1990) The embryonic development of larval muscles in Drosophila. Development 110: 791-804.
31. Maqbool T, Jagla K (2007) Genetic control of muscle development: learning from Drosophila. J Muscle Res Cell Motil 28: 397-407.
32. Beckett K, Baylies MK (2006) The development of the Drosophila larval body wall muscles. Int Rev Neurobiol 75: 55-70.
33. Raghavan KV, Pinto L (1985) The cell lineage of the muscles of the Drosophila head. J Embryol Exp Morphol 85: 285-294.
34. Hartenstein V (1993) Atlas of Drosophila Development. Cold Spring Harbor Laboratory Press.
35. Fernandes J, Bate M, Vijayraghavan K (1991) Development of the indirect flight muscles of Drosophila. Development 113: 67-77.
36. Eldred CC, Simeonov DR, Koppes RA, Yang C, Corr DT, et al. (2010) The mechanical properties of Drosophila jump muscle expressing wild-type and embryonic Myosin isoforms. Biophys J 98: 1218-1226.
37. Currie DA, Bate M (1991) The development of adult abdominal muscles in Drosophila: myoblasts express twist and are associated with nerves. Development 113: 91-102.
38. Koenig JH, Ikeda K (2005) Relationship of the reserve vesicle population to synaptic depression in the tergotrochanteral and dorsal longitudinal muscles of Drosophila. J Neurophysiol 94: 2111-2119.

39. Schonbauer C, Distler J, Jahrling N, Radolf M, Dodt HU, et al. (2011) Spalt mediates an evolutionarily conserved switch to fibrillar muscle fate in insects. Nature 479: 406-409.
40. Soler C, Daczewska M, Da Ponte JP, Dastugue B, Jagla K (2004) Coordinated development of muscles and tendons of the Drosophila leg. Development 131: 6041-6051.
41. Piazza N, Gosangi B, Devilla S, Arking R, Wessells R (2009) Exercise-training in young Drosophila melanogaster reduces age-related decline in mobility and cardiac performance. PLoS One 4: e5886.
42. Piazza N, Wessells RJ (2011) Drosophila models of cardiac disease. Prog Mol Biol Transl Sci 100: 155-210.
43. Littlefield R, Fowler VM (1998) Defining actin filament length in striated muscle: rulers and caps or dynamic stability? Annu Rev Cell Dev Biol 14: 487-525.
44. Fyrberg E (1989) Study of contractile and cytoskeletal proteins using Drosophila genetics. Cell Motil Cytoskeleton 14: 118-127.
45. Vigoreaux JO (2001) Genetics of the Drosophila flight muscle myofibril: a window into the biology of complex systems. Bioessays 23: 1047-1063.
46. Maughan DW, Vigoreaux JO (1999) An Integrated View of Insect Flight Muscle: Genes, Motor Molecules, and Motion. News Physiol Sci 14: 87-92.
47. Bullard B, Burkart C, Labeit S, Leonard K (2005) The function of elastic proteins in the oscillatory contraction of insect flight muscle. J Muscle Res Cell Motil 26: 479-485.
48. Josephson RK, Malamud JG, Stokes DR (2000) Asynchronous muscle: a primer. J Exp Biol 203: 2713-2722.
49. Burkart C, Qiu F, Brendel S, Benes V, Haag P, et al. (2007) Modular proteins from the Drosophila sallimus (sls) gene and their expression in muscles with different extensibility. J Mol Biol 367: 953-969.
50. Fyrberg CC, Labeit S, Bullard B, Leonard K, Fyrberg E (1992) Drosophila projectin: relatedness to titin and twitchin and correlation with lethal(4) 102 CDa and bent-dominant mutants. Proc Biol Sci 249: 33-40.
51. Sparrow J, Hughes SM, Segalat L (2008) Other model organisms for sarcomeric muscle diseases. Adv Exp Med Biol 642: 192-206.
52. Rando TA (2002) Oxidative stress and the pathogenesis of muscular dystrophies. Am J Phys Med Rehabil 81: S175-186.
53. Greene JC, Whitworth AJ, Andrews LA, Parker TJ, Pallanck LJ (2005) Genetic and genomic studies of Drosophila parkin mutants implicate oxidative stress and innate immune responses in pathogenesis. Hum Mol Genet 14: 799-811.
54. Greene JC, Whitworth AJ, Kuo I, Andrews LA, Feany MB, et al. (2003) Mitochondrial pathology and apoptotic muscle degeneration in Drosophila parkin mutants. Proc Natl Acad Sci U S A 100: 4078-4083.
55. Vercherat C, Chung TK, Yalcin S, Gulbagci N, Gopinadhan S, et al. (2009) Stra13 regulates oxidative stress mediated skeletal muscle degeneration. Hum Mol Genet 18: 4304-4316.

56. Lazaro RP, Dentinger MP, Rodichok LD, Barron KD, Satya-Murti S (1986) Muscle pathology in Bassen-Kornzweig syndrome and vitamin E deficiency. Am J Clin Pathol 86: 378-387.
57. Kar NC, Pearson CM (1979) Catalase, superoxide dismutase, glutathione reductase and thiobarbituric acid-reactive products in normal and dystrophic human muscle. Clin Chim Acta 94: 277-280.
58. Lloyd TE, Taylor JP (2010) Flightless flies: Drosophila models of neuromuscular disease. Ann N Y Acad Sci 1184: e1-20.
59. Greener MJ, Roberts RG (2000) Conservation of components of the dystrophin complex in Drosophila. FEBS Lett 482: 13-18.
60. van der Plas MC, Pilgram GS, de Jong AW, Bansraj MR, Fradkin LG, et al. (2007) Drosophila Dystrophin is required for integrity of the musculature. Mech Dev 124: 617-630.
61. Allikian MJ, Bhabha G, Dospoy P, Heydemann A, Ryder P, et al. (2007) Reduced life span with heart and muscle dysfunction in Drosophila sarcoglycan mutants. Hum Mol Genet 16: 2933-2943.
62. Haigh SE, Salvi SS, Sevdali M, Stark M, Goulding D, et al. (2010) Drosophila indirect flight muscle specific Act88F actin mutants as a model system for studying congenital myopathies of the human ACTA1 skeletal muscle actin gene. Neuromuscul Disord 20: 363-374.
63. Schnorrer F, Schonbauer C, Langer CC, Dietzl G, Novatchkova M, et al. (2010) Systematic genetic analysis of muscle morphogenesis and function in Drosophila. Nature 464: 287-291.
64. Berthier C, Blaineau S (1997) Supramolecular organization of the subsarcolemmal cytoskeleton of adult skeletal muscle fibers. A review. Biol Cell 89: 413-434.
65. Reedy MC, Beall C (1993) Ultrastructure of developing flight muscle in Drosophila. I. Assembly of myofibrils. Dev Biol 160: 443-465.
66. Hein S, Kostin S, Heling A, Maeno Y, Schaper J (2000) The role of the cytoskeleton in heart failure. Cardiovasc Res 45: 273-278.
67. Peckham M (2008) Engineering a multi-nucleated myotube, the role of the actin cytoskeleton. J Microsc 231: 486-493.
68. Tskhovrebova L, Trinick J (2003) Titin: properties and family relationships. Nat Rev Mol Cell Biol 4: 679-689.
69. Crawford GL, Horowits R (2011) Scaffolds and chaperones in myofibril assembly: putting the striations in striated muscle. Biophys Rev 3: 25-32.
70. Kronert WA, O'Donnell PT, Fieck A, Lawn A, Vigoreaux JO, et al. (1995) Defects in the Drosophila myosin rod permit sarcomere assembly but cause flight muscle degeneration. J Mol Biol 249: 111-125.
71. Barton B, Ayer G, Maughan DW, Vigoreaux JO (2007) Site directed mutagenesis of Drosophila flightin disrupts phosphorylation and impairs flight muscle structure and mechanics. J Muscle Res Cell Motil 28: 219-230.
72. Contompasis JL, Nyland LR, Maughan DW, Vigoreaux JO (2010) Flightin is necessary for length determination, structural integrity, and large bending stiffness of insect flight muscle thick filaments. J Mol Biol 395: 340-348.

73. Nongthomba U, Cummins M, Clark S, Vigoreaux JO, Sparrow JC (2003) Suppression of muscle hypercontraction by mutations in the myosin heavy chain gene of Drosophila melanogaster. Genetics 164: 209-222.
74. Thornhill P, Bassett D, Lochmuller H, Bushby K, Straub V (2008) Developmental defects in a zebrafish model for muscular dystrophies associated with the loss of fukutin-related protein (FKRP). Brain 131: 1551-1561.
75. Perkins AD, Ellis SJ, Asghari P, Shamsian A, Moore ED, et al. (2010) Integrin-mediated adhesion maintains sarcomeric integrity. Dev Biol 338: 15-27.
76. Clarkson E, Costa CF, Machesky LM (2004) Congenital myopathies: diseases of the actin cytoskeleton. J Pathol 204: 407-417.
77. Hackman P, Vihola A, Haravuori H, Marchand S, Sarparanta J, et al. (2002) Tibial muscular dystrophy is a titinopathy caused by mutations in TTN, the gene encoding the giant skeletal-muscle protein titin. Am J Hum Genet 71: 492-500.
78. Salmikangas P, van der Ven PF, Lalowski M, Taivainen A, Zhao F, et al. (2003) Myotilin, the limb-girdle muscular dystrophy 1A (LGMD1A) protein, cross-links actin filaments and controls sarcomere assembly. Hum Mol Genet 12: 189-203.
79. Ranganayakulu B, Ravikumar GP, Bhaskar AV (1998) Battered child syndrome. Indian J Dermatol Venereol Leprol 64: 245-246.
80. Ranganayakulu B, Ravikumar GP, Bhaskar GV (1998) Ano-rectal involvement in lymphogranuloma venereum. Indian J Dermatol Venereol Leprol 64: 187-188.
81. Zak R, Martin AF, Prior G, Rabinowitz M (1977) Comparison of turnover of several myofibrillar proteins and critical evaluation of double isotope method. J Biol Chem 252: 3430-3435.
82. Terui T, Sodnomtseren M, Matsuba D, Udaka J, Ishiwata S, et al. (2008) Troponin and titin coordinately regulate length-dependent activation in skinned porcine ventricular muscle. J Gen Physiol 131: 275-283.
83. Bassett DI, Currie PD (2003) The zebrafish as a model for muscular dystrophy and congenital myopathy. Hum Mol Genet 12 Spec No 2: R265-270.
84. Beall CJ, Fyrberg E (1991) Muscle abnormalities in Drosophila melanogaster heldup mutants are caused by missing or aberrant troponin-I isoforms. J Cell Biol 114: 941-951.
85. Deconinck AE, Rafael JA, Skinner JA, Brown SC, Potter AC, et al. (1997) Utrophin-dystrophin-deficient mice as a model for Duchenne muscular dystrophy. Cell 90: 717-727.
86. Pai AC (1965) Developmental Genetics of a Lethal Mutation, Muscular Dysgenesis (Mdg), in the Mouse. I. Genetic Analysis and Gross Morphology. Dev Biol 11: 82-92.
87. Goldstein LS, Gunawardena S (2000) Flying through the drosophila cytoskeletal genome. J Cell Biol 150: F63-68.
88. Roper K, Mao Y, Brown NH (2005) Contribution of sequence variation in Drosophila actins to their incorporation into actin-based structures in vivo. J Cell Sci 118: 3937-3948.
89. Leal SM, Neckameyer WS (2002) Pharmacological evidence for GABAergic regulation of specific behaviors in Drosophila melanogaster. J Neurobiol 50: 245-261.
90. Schmittgen TD, Livak KJ (2008) Analyzing real-time PCR data by the comparative C(T) method. Nat Protoc 3: 1101-1108.

91. Miller MS, Lekkas P, Braddock JM, Farman GP, Ballif BA, et al. (2008) Aging enhances indirect flight muscle fiber performance yet decreases flight ability in Drosophila. Biophys J 95: 2391-2401.
92. Karlik CC, Coutu MD, Fyrberg EA (1984) A nonsense mutation within the act88F actin gene disrupts myofibril formation in Drosophila indirect flight muscles. Cell 38: 711-719.
93. Fyrberg EA, Goldstein LS (1990) The Drosophila cytoskeleton. Annu Rev Cell Biol 6: 559-596.
94. Udaka J, Ohmori S, Terui T, Ohtsuki I, Ishiwata S, et al. (2008) Disuse-induced preferential loss of the giant protein titin depresses muscle performance via abnormal sarcomeric organization. J Gen Physiol 131: 33-41.
95. Ottenheijm CA, Witt CC, Stienen GJ, Labeit S, Beggs AH, et al. (2009) Thin filament length dysregulation contributes to muscle weakness in nemaline myopathy patients with nebulin deficiency. Hum Mol Genet 18: 2359-2369.
96. Tanner BC, Miller MS, Miller BM, Lekkas P, Irving TC, et al. (2011) COOH-terminal truncation of flightin decreases myofilament lattice organization, cross-bridge binding, and power output in Drosophila indirect flight muscle. Am J Physiol Cell Physiol 301: C383-391.
97. Wells L, Edwards KA, Bernstein SI (1996) Myosin heavy chain isoforms regulate muscle function but not myofibril assembly. EMBO J 15: 4454-4459.
98. Ono S (2010) Dynamic regulation of sarcomeric actin filaments in striated muscle. Cytoskeleton (Hoboken) 67: 677-692.
99. Chen EH, Pryce BA, Tzeng JA, Gonzalez GA, Olson EN (2003) Control of myoblast fusion by a guanine nucleotide exchange factor, loner, and its effector ARF6. Cell 114: 751-762.
100. Schnorrer F, Kalchhauser I, Dickson BJ (2007) The transmembrane protein Kon-tiki couples to Dgrip to mediate myotube targeting in Drosophila. Dev Cell 12: 751-766.
101. Bai J, Binari R, Ni JQ, Vijayakanthan M, Li HS, et al. (2008) RNA interference screening in Drosophila primary cells for genes involved in muscle assembly and maintenance. Development 135: 1439-1449.
102. Yuan L, Fairchild MJ, Perkins AD, Tanentzapf G (2010) Analysis of integrin turnover in fly myotendinous junctions. J Cell Sci 123: 939-946.
103. Reedy MC, Bullard B, Vigoreaux JO (2000) Flightin is essential for thick filament assembly and sarcomere stability in Drosophila flight muscles. J Cell Biol 151: 1483-1500.
104. Arbeitman MN, Furlong EE, Imam F, Johnson E, Null BH, et al. (2002) Gene expression during the life cycle of Drosophila melanogaster. Science 297: 2270-2275.
105. da Silva Lopes K, Pietas A, Radke MH, Gotthardt M (2011) Titin visualization in real time reveals an unexpected level of mobility within and between sarcomeres. J Cell Biol 193: 785-798.
106. LaGrange BM, Low RB (1976) Turnover of myosin heavy and light chains in cultured embryonic chick cardiac and skeletal muscle. Dev Biol 54: 214-229.
107. Ghosh SR, Hope IA (2010) Determination of the mobility of novel and established Caenorhabditis elegans sarcomeric proteins in vivo. Eur J Cell Biol 89: 437-448.

108. Wang J, Shaner N, Mittal B, Zhou Q, Chen J, et al. (2005) Dynamics of Z-band based proteins in developing skeletal muscle cells. Cell Motil Cytoskeleton 61: 34-48.
109. Gargano JW, Martin I, Bhandari P, Grotewiel MS (2005) Rapid iterative negative geotaxis (RING): a new method for assessing age-related locomotor decline in Drosophila. Exp Gerontol 40: 386-395.
110. Rhodenizer D, Martin I, Bhandari P, Pletcher SD, Grotewiel M (2008) Genetic and environmental factors impact age-related impairment of negative geotaxis in Drosophila by altering age-dependent climbing speed. Exp Gerontol 43: 739-748.
111. Spence HJ, Chen YJ, Winder SJ (2002) Muscular dystrophies, the cytoskeleton and cell adhesion. Bioessays 24: 542-552.
112. Engel AG (2008) The neuromuscular junction. Handb Clin Neurol 91: 103-148.
113. Hu S, Fambrough D, Atashi JR, Goodman CS, Crews ST (1995) The Drosophila abrupt gene encodes a BTB-zinc finger regulatory protein that controls the specificity of neuromuscular connections. Genes Dev 9: 2936-2948.
114. Wucherpfennig T, Wilsch-Brauninger M, Gonzalez-Gaitan M (2003) Role of Drosophila Rab5 during endosomal trafficking at the synapse and evoked neurotransmitter release. J Cell Biol 161: 609-624.
115. Laviolette MJ, Nunes P, Peyre JB, Aigaki T, Stewart BA (2005) A genetic screen for suppressors of Drosophila NSF2 neuromuscular junction overgrowth. Genetics 170: 779-792.
116. Anderson PR, Kirby K, Hilliker AJ, Phillips JP (2005) RNAi-mediated suppression of the mitochondrial iron chaperone, frataxin, in Drosophila. Hum Mol Genet 14: 3397-3405.
117. Chen J, Shi X, Padmanabhan R, Wang Q, Wu Z, et al. (2008) Identification of novel modulators of mitochondrial function by a genome-wide RNAi screen in Drosophila melanogaster. Genome Res 18: 123-136.
118. Copeland JM, Cho J, Lo T, Jr., Hur JH, Bahadorani S, et al. (2009) Extension of Drosophila life span by RNAi of the mitochondrial respiratory chain. Curr Biol 19: 1591-1598.
119. Miller MK, Granzier H, Ehler E, Gregorio CC (2004) The sensitive giant: the role of titin-based stretch sensing complexes in the heart. Trends Cell Biol 14: 119-126.
120. Katzemich A, Kreiskother N, Alexandrovich A, Elliott C, Schock F, et al. (2012) The function of the M-line protein obscurin in controlling the symmetry of the sarcomere in the flight muscle of Drosophila. J Cell Sci 125: 3367-3379.
121. Herzog JA, Leonard TR, Jinha A, Herzog W (2012) Are titin properties reflected in single myofibrils? J Biomech 45: 1893-1899.
122. Fraterman S, Zeiger U, Khurana TS, Wilm M, Rubinstein NA (2007) Quantitative proteomics profiling of sarcomere associated proteins in limb and extraocular muscle allotypes. Mol Cell Proteomics 6: 728-737.
123. Seto JT, Chan S, Turner N, MacArthur DG, Raftery JM, et al. (2011) The effect of alpha-actinin-3 deficiency on muscle aging. Exp Gerontol 46: 292-302.
124. Stewart M, Hogg N (1996) Regulation of leukocyte integrin function: affinity vs. avidity. J Cell Biochem 61: 554-561.
125. Hogg N, Bates PA (2000) Genetic analysis of integrin function in man: LAD-1 and other syndromes. Matrix Biol 19: 211-222.

126. Scales TM, Parsons M (2011) Spatial and temporal regulation of integrin signalling during cell migration. Curr Opin Cell Biol 23: 562-568.

Appendices

Appendix A - Using 'R' the generate heatmaps

The following script can be used in 'R' to generate the heatmaps presented in Figure 3.4 and Figure 3.5. This script was adapted from a freely-available template script posted online at E-Notações (http://enotacoes.wordpress.com/2007/11/16/easy-guide-to-drawing-heat-maps-to-pdf-with-r-with-color-key/).

```
#heatmap generation script

setwd("/Users/~")
library(RColorBrewer)
library(gplots)
x=read.table("matrix_adj.dat", header=TRUE)
mat=data.matrix(x)

pdf("heatmap.pdf", height=10, width=10)
heatmap.2(mat,
Rowv=TRUE,
Colv=TRUE,
#    dendrogram= c("none"),
distfun = dist,
hclustfun = hclust,
xlab = "X data", ylab = "Y data",
key=TRUE,
keysize=1,
trace="none",
density.info=c("none"),
margins=c(10, 8),
col=brewer.pal(11,"PiYG")
#    col=redgreen(75),
 )
dev.off()
```

Appendix B - Statistical analysis for negative geotaxis assays

The following is supporting material for

B.1 'R' Script for analyzing negative geotaxis assay data

The following script was used to analyze the data gathered from the negative geotaxis assays. It generates, using the GEE approach, the estimated values X, Y, and Z for Equation 1 (see Section 2.5 Negative geotaxis assay and Section 2.6 Statistical modeling of the negative geotaxis assay data)

```
##Statistical analysis script

#set the directory
setwd("/Users/~")
#read the data file
library(xlsx)
#Your data file was processed within the excel file in order to
be analyzed in R.
#Please see the data file sent from Tara
data <- read.xlsx("all data clean adj.xlsx", sheetIndex = 1,
colIndex = 1:6, rowIndex = 1:5446,
as.data.frame=TRUE, stringsAsFactors = FALSE)
#Remove the data that is NA.
adj_data <- data
names(adj_data) <- c("Prop", "Day", "Gene","ID","Success",
"Failure")

#A convenient way to make control group as the reference group
c_index <- which(adj_data$Gene == "Control")
adj_data$Gene[c_index] = "aaControl"
#make Gene as a factor
adj_data$Gene <- as.factor(adj_data$Gene)
#check number of different types of Gene
levels(adj_data$Gene)
length(levels(adj_data$Gene))
#Make ID as a factor
adj_data$ID <- as.factor(adj_data$ID)
#number of batches
levels(adj_data$ID)

library("geepack")
library("gee")
```

```
#fitting a GEE model
gee.fit4 <- geeglm(cbind(Success, Failure) ~ Gene + Day +
I(Day*Day) +
Day*Gene + I(Day*Day)*Gene, data = adj_data, family =
"binomial", id = ID, corstr = "ar1")
summary(gee.fit4)
## print the GEE outputs
x <- as.matrix(summary(gee.fit4)$coefficients)
y <- matrix(as.numeric(sprintf("%.4f", x)), ncol = ncol(x))
dimnames(y) <- dimnames(x)
print(y)
#plot fitted proportions against the observed proportion of
flies climbing above
#the experimental line
pred <- gee.fit4$fitted.values
obs_prob <- adj_data$Success/(adj_data$Success +
adj_data$Failure)
plot(obs_prob, pred, main = "Fitted Probability against Obseved
Probability",
xlab = "Observed Probability of flies climbing above the
experimental line",
ylab = "Predicted Probability of flies climbing above the
experimental line")
# 45 degrees line
abline(0,1)
dev.print(device = postscript, file = "geediag.ps", horizontal =
FALSE)
# approximate 95% confidence intervals for logit p at a given
day
library(doBy)
obs_day <- seq(0, 30, by = 3)


#evaluate odds on Days 0 to 30 for flies with GeneX knocked-out
#and its corresponding approximate 95 % CI.
#"esticon" plugs the values of the predictors to the fitted
model. It computes the linear
#function of the estimated regression parameters and its
corresponding 95% CI.
# cm is for specifying linear combinations of parameters in
order to
# get the estimated odds and CIs.

odds_mat <- sapply(1:length(obs_day), function(x)[
esticon(gee.fit4, cm =c(1, rep(0,1), 1, rep(0,154), obs_day[x],
obs_day[x]*obs_day[x], rep(0,1), obs_day[x], rep(0,154),
rep(0,1), obs_day[x]*obs_day[x], rep(0,154)) ) ])
```

```
#logit p
GeneXlogit <- unlist(odds_mat[2,])
#odds
odds <- exp(GeneXlogit)
#the upper bound of the 95% confidence intervals for flies with
gene GeneX knocked-out
GeneX_up <- exp(unlist(odds_mat[8,]))
#the lower bound of the 95% confidence intervals for flies with
gene GeneX knocked-out
GeneX_lw <- exp(unlist(odds_mat[7,]))
plot(obs_day, odds, xlab = "Day",
ylab = "Fitted odds of Successfully climbing above the
experimental line",
main = "Fitted odds for GeneX gene knocked-out flies", ylim =
c(-1, 14))
lines( x = rep(obs_day[1],2) ,y = c(GeneX_lw[1], GeneX_up[1])
,col = "red", type="l")
lines( x = rep(obs_day[2],2) ,y = c(GeneX_lw[2], GeneX_up[2])
,col = "red", type="l")
lines( x = rep(obs_day[3],2) ,y = c(GeneX_lw[3], GeneX_up[3])
,col = "red", type="l")
lines( x = rep(obs_day[4],2) ,y = c(GeneX_lw[4], GeneX_up[4])
,col = "red", type="l")
lines( x = rep(obs_day[5],2) ,y = c(GeneX_lw[5], GeneX_up[5])
,col = "red", type="l")
lines( x = rep(obs_day[6],2) ,y = c(GeneX_lw[6], GeneX_up[6])
,col = "red", type="l")
lines( x = rep(obs_day[7],2) ,y = c(GeneX_lw[7], GeneX_up[7])
,col = "red", type="l")
lines( x = rep(obs_day[8],2) ,y = c(GeneX_lw[8], GeneX_up[8])
,col = "red", type="l")
dev.print(device = postscript, file = "GeneXodds.ps", horizontal
= FALSE)
#evaluate odds on Days 0 to 30 for flies in the control group
#and its corresponding approximate 95 % CI.
# cm is for specifying linear combinations of parameters
#in order to get the estimated odds and CIs.
codds_mat <- sapply(1:length(obs_day), function(x){
esticon(gee.fit4,
cm =c(1, 0, rep(0, 155), obs_day[x], obs_day[x]*obs_day[x],
0,rep(0, 155), 0,
rep(0, 155))  )  })

#logit p
clogit <- unlist(codds_mat[2,])
```

```
#odds
codds <- exp(clogit)
#the upper bound of the 95% confidence intervals for control
flies
c_up <- exp(unlist(codds_mat[8,]))
#the lower bound of the 95% confidence intervals for control
flies
c_lw <- exp(unlist(codds_mat[7,]))
plot(obs_day, codds, xlab = "Day",
ylab = "Fitted odds of Successfully climbing above the
experimental line",
main = "Fitted odds for flies in the Control", ylim = c(-1, 14))
lines( x = rep(obs_day[1],2) ,y = c(c_lw[1], c_up[1]) ,col =
"red", type="l")
lines( x = rep(obs_day[2],2) ,y = c(c_lw[2], c_up[2]) ,col =
"red", type="l")
lines( x = rep(obs_day[3],2) ,y = c(c_lw[3], c_up[3]) ,col =
"red", type="l")
lines( x = rep(obs_day[4],2) ,y = c(c_lw[4], c_up[4]) ,col =
"red", type="l")
lines( x = rep(obs_day[5],2) ,y = c(c_lw[5], c_up[5]) ,col =
"red", type="l")
lines( x = rep(obs_day[6],2) ,y = c(c_lw[6], c_up[6]) ,col =
"red", type="l")
lines( x = rep(obs_day[7],2) ,y = c(c_lw[7], c_up[7]) ,col =
"red", type="l")
lines( x = rep(obs_day[8],2) ,y = c(c_lw[8], c_up[8]) ,col =
"red", type="l")
dev.print(device = postscript, file = "codds.ps", horizontal =
FALSE)
#Comparing flies with gene GeneX knocked-out
#relative to flies in the control group by odds ratio
# odds ratio
or <- exp(GeneXlogit)/exp(clogit)
#create a matrix to store the output for log odds ratio
log_or = matrix(NA, nrow = 8, ncol = length(obs_day))
for(jj in 1:length(obs_day)){
#linear combination of parameters for the control group
cm_control = c(1, 0, rep(0, 155), obs_day[jj],
obs_day[jj]*obs_day[jj], 0,rep(0, 155), 0,
rep(0, 155))

#linear combinations of parameters for the GeneX group
cm_GeneX = c(1, rep(0,1), 1, rep(0,154), obs_day[jj],
obs_day[jj]*obs_day[jj], rep(0,1), obs_day[jj], rep(0,154),
rep(0,1), obs_day[jj]*obs_day[jj], rep(0,154))
```

```
#the difference of the linear combinations of parameters for two
groups of flies.
cm_or = cm_GeneX - cm_control
#log odds ratio and their confidence intervals
log_or[,jj] = unlist(esticon(gee.fit4,cm = cm_or))
}
#convert the confidence intervals to the odds ratio scale
exp_lw <- exp(log_or[7,])
exp_up <- exp(log_or[8,])
#Plot odds ratio and itís estimated confidence intervals
plot(obs_day[-1], or[-1], xlab = "Day", ylab =
"Estimated odds ratio of GeneX knocked-out flies relative to
flies in the control", main = "GeneX",
ylim = c(-1, 2))
#lines( x = rep(obs_day[1],2) ,y = c(exp_lw[1], exp_up[1]) ,col
= "red", type="l")
lines( x = rep(obs_day[2],2) ,y = c(exp_lw[2], exp_up[2]) ,col =
"red", type="l")
lines( x = rep(obs_day[3],2) ,y = c(exp_lw[3], exp_up[3]) ,col =
"red", type="l")
lines( x = rep(obs_day[4],2) ,y = c(exp_lw[4], exp_up[4]) ,col =
"red", type="l")
lines( x = rep(obs_day[5],2) ,y = c(exp_lw[5], exp_up[5]) ,col =
"red", type="l")
lines( x = rep(obs_day[6],2) ,y = c(exp_lw[6], exp_up[6]) ,col =
"red", type="l")
lines( x = rep(obs_day[7],2) ,y = c(exp_lw[7], exp_up[7]) ,col =
"red", type="l")
lines( x = rep(obs_day[8],2) ,y = c(exp_lw[8], exp_up[8]) ,col =
"red", type="l")
dev.print(device = postscript, file = "GeneX.ps", horizontal =

FALSE)
```

B.2 Estimations for X, Y and Z coefficients from the GEE approach for all genes screened in the TARGET screen.

The following table provides the X, Y and Z estimates produced using the ‘R’ script given in Appendix B.1. The X values are the values in the ‘Estimate’ column from the ‘Intercept’ to ‘Genezfh11322’ rows. The Y values are the values in the ‘Geneab4807R:Day’ to ‘Genezhf11322:Day’ rows. The Z values are the values in the ‘Estimate’ column from the

'Geneab4807R:I(Day * Day)' to the 'Genezhf11322:I(Day * Day)' rows. The length of the table makes it impractical to be included here. The relevant file, 'Appendix B2.txt', has been archived online at: https://www.dropbox.com/s/6s14psjro5lsj19/Appendix%20B2.txt.

Appendix C - Datasets of results from the Mef2::GAL4 and TARGET screens

C.1 List of all 271 genes screened

List of all 271 genes screened organized by CG Number. The 'Name' column gives the full name or abbreviation as listed on FlyBase (ww.flybase.org). The 'CG' column gives the CG number, a unique identifier assigned to each fly gene. The 'Collection' column lists the RNAi stock centre from which the line was obtained. NIG is the NIG-Fly Stock Centre (Kyoto, Japan; http://www.shigen.nig.ac.jp/fly/nigfly/index.jsp); VDRC is the Viennese Drosophila RNAi Centre (Vienna, Austria; http://stockcenter.vdrc.at); and TRiP is the Transgenic RNAi Project (Boston, USA; http://www.flyrnai.org/). The 'Collection ID' column lists the unique identifier for each RNAi hairpin construct as assigned by the source Collection. The 'Muscle Classification' and 'Cytoskeletal Classification' columns give broad functional information on the role of the gene as defined by GO terms and the literature (see Materials and Methods). The length of the table makes it impractical to be included here. The relevant file, 'Appendix C1 List of all 271 genes screened' has been archived online at: https://www.dropbox.com/s/8o4u3k7s53x5sqr/Appendix%20C1%20List%20of%20all%20271%20genes%20screened.xlsx.

C.2 Results of the Mef2::GAL4 screen

List of the phenotypes obtained in the Mef2::GAL4 screen. The 'Name' column gives the full name or abbreviation as listed on FlyBase (ww.flybase.org). The 'CG' column gives the CG number, a unique identifier assigned to each fly gene. The 'Collection' column lists the RNAi stock centre from which the line was obtained. NIG is the NIG-Fly Stock Centre (Kyoto, Japan; http://www.shigen.nig.ac.jp/fly/nigfly/index.jsp); VDRC is the Viennese Drosophila RNAi Centre (Vienna, Austria; http://stockcenter.vdrc.at); and TRiP is the Transgenic RNAi Project (Boston, USA; http://www.flyrnai.org/). The 'Collection ID' column lists the unique identifier for each RNAi hairpin construct as assigned by the source Collection. The 'Mef2::GAL4 Phenotype' column lists the phenotypes obtained when the listed gene was knocked-down using the Mef2::GAL4 system (see Materials and Methods). The 'Muscle Classification' and 'Cytoskeletal Classification' columns give broad functional information on the role of the gene as defined by GO terms and the literature (see Materials and Methods). The length of the table makes it impractical to be included here. The relevant file, 'Appendix C2 Results of the Mef2::GAL4 screen' has been archived online at: https://www.dropbox.com/s/iak9oq2pv88yq3n/Appendix%20C2%20Results%20of%20the%20Mef2%3B%3BGAL4%20screen.xlsx.

C.3 Results of the TARGET screen

List of the phenotypes obtained in the Mef2::GAL4 screen. The 'Name' column gives the full name or abbreviation as listed on FlyBase (ww.flybase.org). The 'CG' column gives the CG number, a unique identifier assigned to each fly gene. The 'Collection' column lists the RNAi stock centre from which the line was obtained. NIG is the NIG-Fly Stock Centre (Kyoto, Japan;

http://www.shigen.nig.ac.jp/fly/nigfly/index.jsp); VDRC is the Viennese Drosophila RNAi Centre (Vienna, Austria; http://stockcenter.vdrc.at); and TRiP is the Transgenic RNAi Project (Boston, USA; http://www.flyrnai.org/). The 'Collection ID' column lists the unique identifier for each RNAi hairpin construct as assigned by the source Collection. The 'TARGET Phenotype' column lists the phenotypes obtained when the listed gene was knocked-down using the TARGET system (see Materials and Methods). The 'Phenotype Severity' column lists the time at which flies lost climbing ability when the listed gene was knocked-down. Loss of climbing ability between Day 0 and Day 9 were classed as 'Severe'; between Day 12 and Day 21 were classed as 'Intermediate'; between Day 24 and Day 30 as 'Weak'; and 'No defect' if climbing ability was not lost. The 'Muscle Classification' and 'Cytoskeletal Classification' columns give broad functional information on the role of the gene as defined by GO terms and the literature (see Materials and Methods). The length of the table makes it impractical to be included here. The relevant file, 'Appendix C3 Results of the TARGET screen.xlsx' has been archived online at: https://www.dropbox.com/s/yczh247dszkh48i/Appendix%20C3%20Results%20of%20the%20TARGET%20screen.xlsx.

Appendix D - *rhea* is required to for hemocyte function and morphology

In addition to the research project into the role of the cytoskeleton in muscle maintenance, I also assisted with the TEM analysis of the role of the IAC in hemocytes. Work in vertebrates has long implicated integrins in cell migration in many cell types but one area of particular interest is in the migration of white blood cells (leukocytes)[124-126]. *D. melanogaster* also have blood cells, known as hemocytes. Although it has been long thought that

integrins contribute to hemocyte migration in the fly, their role has remained poorly understood as the phenotypes observed in integrin mutants are mild. Based on our familiarity with the integrin mutant phenotype we hypothesized that this was because previous studies relied on depletion of only the zygotic contribution of integrin and there was enough maternal contribution to prevent a hemocyte migration defect. By depleting both the maternal and zygotic contribution of integrin or talin a more severe phenotype than previously reported was observed. To closely examine hemocytes, I carried out TEM analysis and found that integrin or talin-deficient hemocytes produce enormous, convoluted filopodia (Figure A.1 C-D). when compared with wildtype hemocytes (Figure A.1 A-B).

Figure A.1 Electron micrographs of hemocytes in wild-type and *rhea* flies

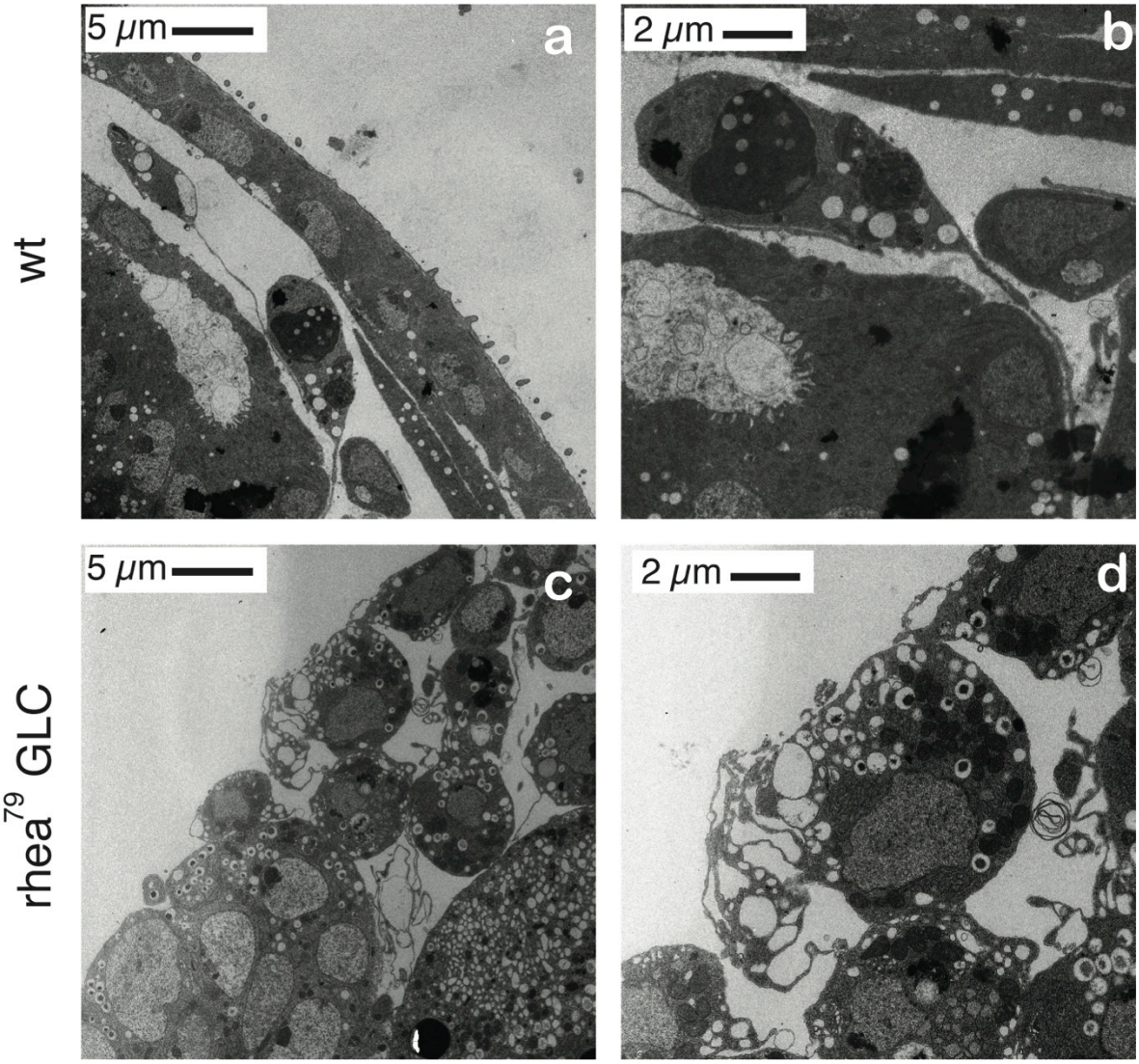

Figure A.1 Electron micrographs of hemocytes in wild-type and *rhea* flies. (a) Hemocytes in a wildtype stage 17 embryos exhibit a simple long filopodial extension (black arrows). (b) A close up of one of the hemocyte in (a). (c) Hemocytes in a talin (M/Z) (mutant stage 17 embryo exhibit a large convoluted, coiled, filopodial extension. (d) A close up of one of the hemocyte in (c). Note the rounded up shape and clustering of the hemocytes in (c) and (d).